Journal Pre-proof

Discovery of Novel c-Mesenchymal-Epithelia Transition Factor and Histone Deacetylase Dual Inhibitors

Hao Hu, Fei Chen, Yuhong Dong, Ming Li, Sicong Xu, Mingze Qin, Ping Gong

PII: S0223-5234(20)30623-1

DOI: https://doi.org/10.1016/j.ejmech.2020.112651

Reference: EJMECH 112651

To appear in: *European Journal of Medicinal Chemistry*

Received Date: 10 January 2020

Revised Date: 6 July 2020

Accepted Date: 7 July 2020

Please cite this article as: H. Hu, F. Chen, Y. Dong, M. Li, S. Xu, M. Qin, P. Gong, Discovery of Novel c-Mesenchymal-Epithelia Transition Factor and Histone Deacetylase Dual Inhibitors, *European Journal of Medicinal Chemistry*, https://doi.org/10.1016/j.ejmech.2020.112651.

Graphical abstract

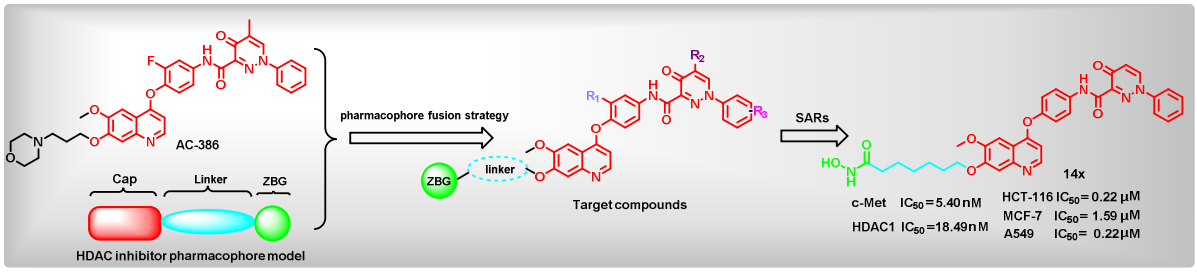

- A series of novel c-Met/HDAC Dual Inhibitors was designed and synthesized.
- **14x** showed potent cytotoxicity against tested cell lines and better enzymatic inhibition.
- Cell apoptosis study revealed **14x** was very effective in the induction of apoptosis in a dose-dependent manner in HCT-116 cells.
- Cell cycle analysis showed that **14x** significantly caused G2/M-phase arrest in HCT-116 cells.
- Docking mode indicated **14x** could form critical bonding interactions with c-Met and HDAC.

Discovery of Novel c-Mesenchymal-Epithelia Transition Factor and Histone Deacetylase Dual Inhibitors

Hao Hu, Fei Chen, Yuhong Dong, Ming Li, Sicong Xu, Mingze Qin*, Ping Gong*[1]

Key Laboratory of Structure-Based Drug Design and Discovery. Ministry of Education, Shenyang Pharmaceutical University, Shenyang 110016, PR China

Abstract

Clinically, a single agent that simultaneously inhibits multiple targets has been widely used in cancer treatment to overcome complicated dose design and anti-cancer resistance. Inspired by the synergistic effects between c-Met and HDAC in tumor development, a novel series of c-Met/HDAC bifunctional inhibitors was designed and synthesized by merging the pharmacophores of HDAC inhibitor into a c-Met inhibitor. All the target compounds were evaluated for their biological activity, the most potent compound, **14x**, exhibited strong inhibition against HDAC1 with an IC_{50} of 18.49 nM and remarkable inhibitory activity against c-Met with an IC_{50} of 5.40 nM, respectively. In addition, **14x** efficiently inhibited the proliferation of HCT-116, MCF-7 and A549 cell lines with IC_{50} values of 0.22 μM, 1.59 μM and 0.22 μM, respectively, which were superior to the reference compounds Cabozantinib and SAHA. Futhermore, **14x** induced apoptosis and cause cell cycle arrest in G2/M phase. Docking experiments on c-Met and HDAC enzymes revealed the key interactions between **14x** with the target protein. These results indicated that **14x** was a potent dual c-Met/HDAC inhibitor and deserved for further investigation.

Keywords: c-Met; HDAC; synthesis; antitumor activity

1. Introduction

c-Mesenchymal-epithelial transition factor (c-Met) is a prototype member of a subfamily of heterodimeric receptor tyrosine kinases (RTKs) which is also known as hepatocyte growth factor receptor (HGFR) [1]. The activation of c-Met by HGF induces several complex signal pathways that result in cell proliferation, survival, motility, angiogenesis and invasion [2-3]. However, the overexpression of HGF has been linked to human cancers, thus c-Met kinase has emerged as a promising target for cancer treatment. During the last few years, several small

[1]Correspondence: Prof. Ping Gong and Mingze Qin, Key Laboratory of Structure-Based Drug Design and Discovery, Ministry of Education, Shenyang Pharmaceutical University, Shenyang 110016, P. R. China.
E-mail: gongpinggp@126.com (P.G.); qinmingze001@126.com (M.Q.)

molecule c-Met kinase inhibitors were under investigation which offered significant therapeutic opportunities for the treatment of tumors. At present, two kinase inhibitors targeting c-Met have been apaproved by Food and Drug Administration (FDA) (**Fig. 1**). Crizotinib, a dual inhibitor of c-Met/ALK kinase, was approved by FDA in August 2011 for the treatment of patients with ALK-positive advanced or metastatic non-small cell lung cancer (NSCLC). Cabozantinib (XL-184), first launched in the U.S in 2013, is used for the treatment of prostate cancer, multiple myeloma, small cell lung cancer and others carcinoma. In 2019, the FDA approved Cabozantinib for patients with advanced hepatocellular carcinoma (HCC) who had been previously treated with Sorafenib [4-5]. However, the current development of c-Met inhibitors is also not going smoothly. Savolitinib, an exquisitely selective c-Met inhibitor, was found with all therapies in the setting for advanced NSCLC with which patients ultimately develop therapeutic resistance [6-8]. Crizotinib case studies had reported on-target c-Met mutations including Y1230H/C, D1228N/H and D1231Y single-point alterations in NSCLC [9]. Although Cabozantinib tend to have a broader activity spectrum to overcome the acquired resistance, an expected increased tolerability burden comparing to Crizotinib and Savolitinib had been indicated [10-11].

Epigenetic aberrations contribute to tumor generation and development. Among the numerous epigenetic enzymes, human histone deacetylases (HDACs) are a family of 18 enzymes that have key effects on numerous cellular functions [12-13]. The over-expression of HDACs is observed in different human cancers, therefore, they are regarded as promising antitumor drug targets [14]. Hence, the developments of HDAC inhibitors are proceeding intensively in academia and pharmaceutical companies. Five HDAC inhibitors have been launched, namely, Vorinostat (SAHA), Romidepsin (FK228), Belinostat (PXD-101), Panobinostat (LBH-589), and Chidamide (**Fig. 1**). In addition, multiple small molecule HDAC inhibitors are also being investigated in clinical trials. Although HDAC inhibitors and other epigenetic agents showed efficacy in hematologic malignancies, challenges still remain in treating against solid tumors [15-17].

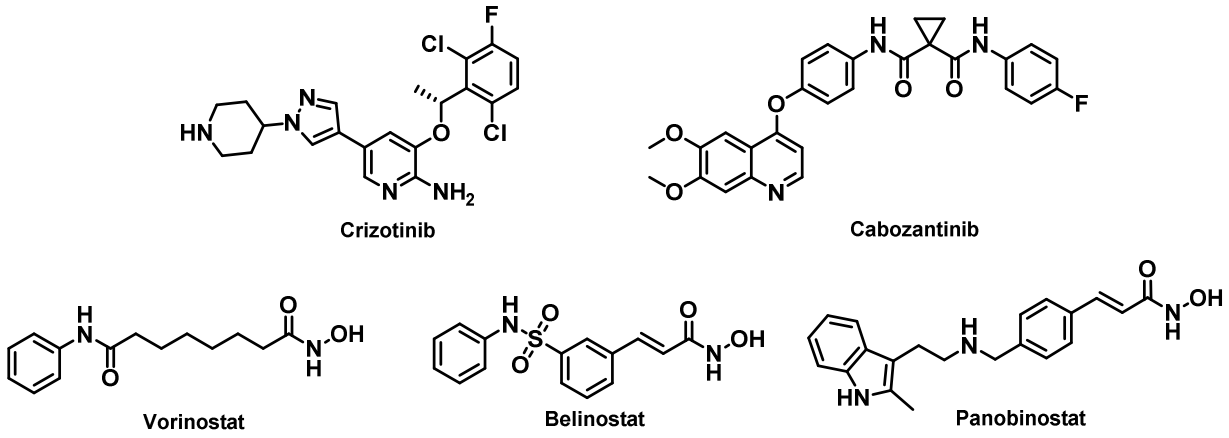

Fig. 1. Structures of several representative c-Met and HDAC inhibitors.

Recently, molecular hybridization paradigm became an interesting and smart way to defeat the multifaceted cancer disease by a single molecular entity that acts via several mechanisms just like a magic bullet. Considerable studies have demonstrated that c-Met and its downstream signaling pathways can be influenced by HDACs both directly and indirectly. In addition, HDACi, which inhibit HGF production [18], can also disrupt the deacetylation of nonhistone proteins such as tubulin, Hsp90, p53, and Bcl-2. Hence, the HDACi can make the pro-growth/pro-survival client proteins (e.g., Raf, AKT, c-Src, etc.) degradation [19-21]. As part of the ongoing research, we decided to design and synthesize a serial of dual c-Met/HDAC inhibitors, with the aim of achieving multitargeted therapy to overcome anti-cancer resistance.

2. Results and discussion

2.1. In silico analysis and design of compounds

In our previous study, we found a compound AC-386 [22] through an in-house high-throughput screening. By using a molecular docking study, we found that the quinoline and pyridazinone moiety of the AC-386 occupy the hinge region of the ATP binding site to form two hydrogen bonds with the residues of c-Met protein. Furthermore, the NH of amide bond form one hydrogen bond with Asp1222 residues (**Fig. 2**). Therefore, the modifications of both two moieties could not be well tolerated. Noting that the substituent at C_7 of the quinoline moiety extends into the solvent exposed region of the protein, which suggested that this site can be modified. Besides, most of HDAC inhibitors share a general pharmacophore comprising three parts (**Fig. 3**), a zinc binding group, a hydrophobic linker and a surface recognition cap [23]. For the classic pharmacophoric model of HDAC inhibitors, the zinc binding group (ZBG) is the most important part of HDAC inhibitors, in which hydroxamic acid and ortho-aminoanilide are the two privileged zinc binding groups [24]. In addition, compounds possessing a hydrazide moiety as the zinc binding group have also been reported [25-26]. Based on our previous molecular docking study, we incorporated hydroxamic acid functionality into C_7 of the quinoline pharmacophore of c-Met inhibitors with a proper spacer expect to obtain dual c-Met/HDAC inhibitors. Inspired by the aforementioned evidence, using pharmacophore fusion strategy, novel hydroxamic dual c-Met/HDAC inhibitors were rationally designed and synthesized (**Fig. 3**).

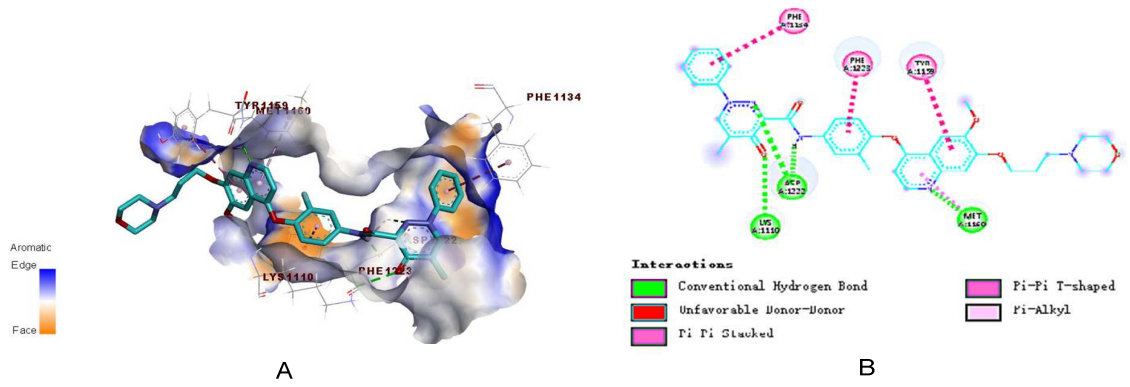

Fig. 2. (A) Proposed binding mode of AC-386 in the ATP pocket of c-Met (PDB code 3LQ8). (B) 2D molecular docking model of AC-386 with protein crystal structure of c-Met.

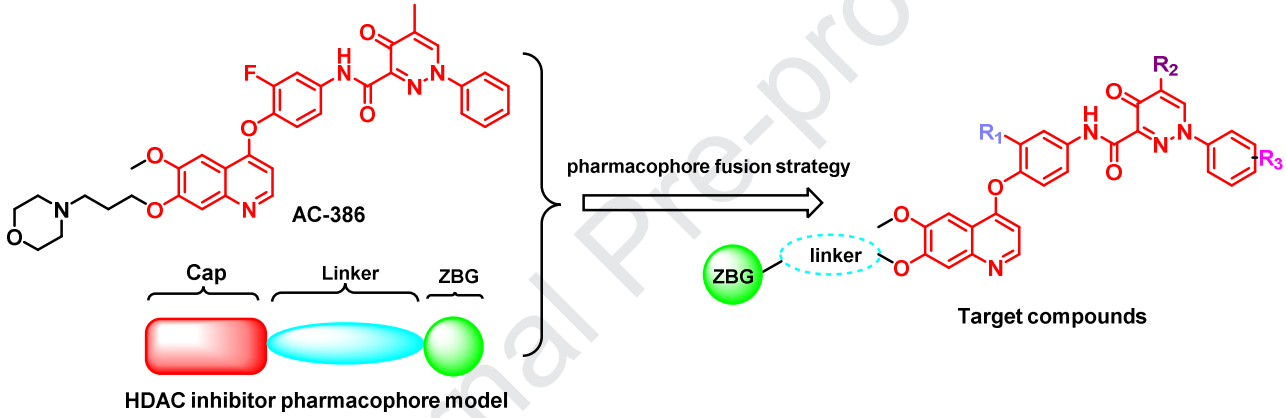

Fig. 3. Design strategy of dual c-Met/HDAC inhibitors.

2.2. Chemistry

*2.2.1. Synthesis of target compounds **14a-14y**.*

The synthetic route to obtain the desired target compounds (**Scheme 1**) is given in the following: the key intermediates **8a-8g** were treated with intermediates **12a-12m** to give condensed amide products **13a-13y**, which were then ammoniated via NH_2OH in dry methanol to give the target hydroxamic acid compounds **14a-14y** [27].

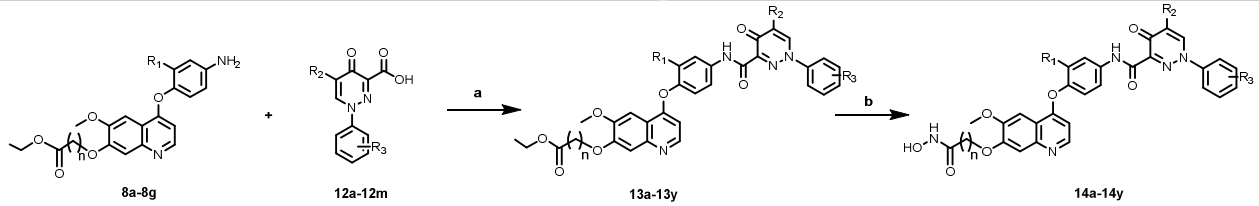

13a,14a:n=1,R_1=H,R_2=H,R_3=2-CF_3 13b,14b:n=1,R_1=H,R_2=CH_3,R_3=3-CF_3,4-Cl 13c,14c:n=1,R_1=H,R_2=CH_3,R_3=2-CH_3 13d,14d:n=3,R_1=F,R_2=CH_3,R_3=2-CH_3 13e,14e:n=3,R_1=F,R_2=CH_3,R_3=H

13f,14f:n=3,R_1=F,R_2=H,R_3=2-CH_3 13g,14g:n=3,R_1=F,R_2=CH_3,R_3=2-F 13h,14h:n=3,R_1=H,R_2=CH_3,R_3=2-F 13i,14i:n=3,R_1=H,R_2=CH_3,R_3=2-CH_3 13j,14j:n=3,R_1=H,R_2=H,R_3=H

13k,14k:n=5,R_1=F,R_2=CH_3,R_3=2-F 13l,14l:n=5,R_1=F,R_2=CH_3,R_3=H 13m,14m:n=5,R_1=H,R_2=H,R_3=2-CH_3 13n,14n:n=5,R_1=H,R_2=CH_3,R_3=2-CH_3 13o,14o:n=6,R_1=H,R_2=CH_3,R_3=H

13p,14p:n=6,R_1=H,R_2=CH_3,R_3=2-CH_3 13q,14q:n=6,R_1=H,R_2=CH_3,R_3=3-Cl,4-F 13r,14r:n=6,R_1=H,R_2=CH_3,R_3=2,4-$2CH_3$ 13s,14s:n=6,R_1=H,R_2=CH_3,R_3=3-CF_3 13t,14t:n=6,R_1=F,R_2=CH_3,R_3=2-CH_3

13u,14u:n=6,R_1=F,R_2=H,R_3=2-CH_3 13v,14v:n=6,R_1=H,R_2=CH_3,R_3=3-CH_3 13w,14w:n=6,R_1=H,R_2=CH_3,R_3=4-CH_3 13x,14x:n=6,R_1=H,R_2=H,R_3=H 13y,14y:n=6,R_1=H,R_2=CH_2CH_3,R_3=H

Scheme 1. Preparation of derivatives of **14a-14y**. Reagents and conditions: (a): HATU, Et_3N, DCM, 40 □, 3-5 h; (b): $NH_2OH{\cdot}HCl$, NaOH, anhydrous, CH_3OH, rt, 2-6 h;

The synthesis of key intermediates **8a-8g** is summarized in **Scheme 2.** Commercially available acetovanillone **1** reacted with different bromo esters to afford **2a-2d**, which were treated with fuming nitric acid to obtain **3a-3d**, respectively. Treating **3a-3d** with DMF-DMA provided **4a-4d**, which were cyclized to give intermediates **5a-5d**, respectively. After chlorination of quinolin-4(1*H*)-one **5a-5d**, the desired intermediates **6a-6d** were obtained. **7a-7g** were obtained through nucleophilic substitution with *p*-nitrophenol or 2-fluoro-4-nitrophenol in chlorobenzene, which were reduced by H_2/Pd to yield the desired intermediates **8a-8g**.

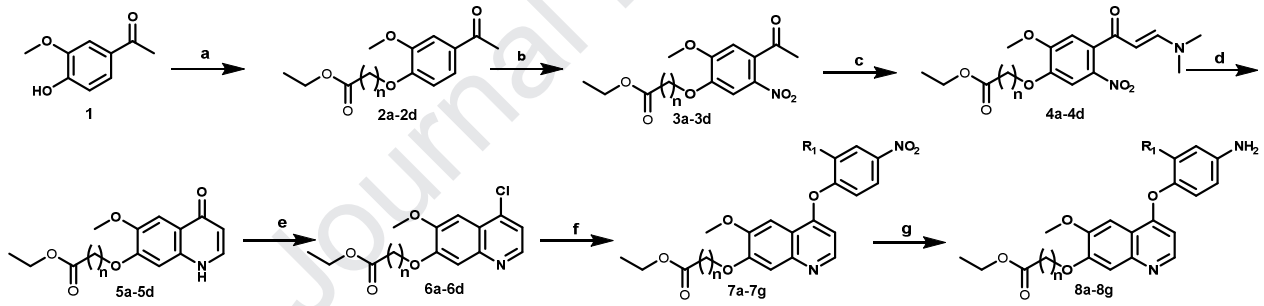

2a,3a,4a,5a,6a:n=1 **2b,3b,4b,5b,6b:n=3** **2c,3c,4c,5c,6c:n=5** **2d,3d,4d,5d,6d:n=6** **7a,8a: n=1,R_1=H**

7b,8b: n=3,R_1=H **7c,8c: n=3,R_1=F** **7d,8d: n=5,R_1=H** **7e,8e: n=5,R_1=F** **7f,8f: n=6,R_1=H** **7g,8g: n=6,R_1=F**

Scheme 2. Preparation of intermediates **8a-8g.** Reagents and conditions: (a) different bromo esters, K_2CO_3, DMF, 80 □, 3-4 h; (b) fuming HNO_3, anhydrous DCM, -5 □, 6-8 h; (c) DMF-DMA, toluene, 110 °C, 7-8 h; (d) Fe powder, AcOH, r.t, 30 min, 80 °C, 1-2 h; (e) $POCl_3$, 85 □, 6-7 h; (f) 2-fluoro-4-nitrophenol/*p*-nitrophenol, PhCl, 140 □, 20-24 h; (g) H_2, Pd/C(10%),CH_3OH, 40 □, 3-5 h.

The substituted dihydropyridazine-4-carboxylic acid **12a-12m,** which were used for the central amidation step as described in **Scheme 3** [28-30] were prepared from the corresponding substituted anilines **9a-9j**. Azo ester intermediates **10a-10m** were obtained from benzenediazonium chloride by reaction with different ethyl acyl acetate, which were reacted with DMF-DMA *via* cyclization to obtained **11a-11m**. The cleavage of the ethyl esters **11a-11m** with NaOH provided **12a-12m**.

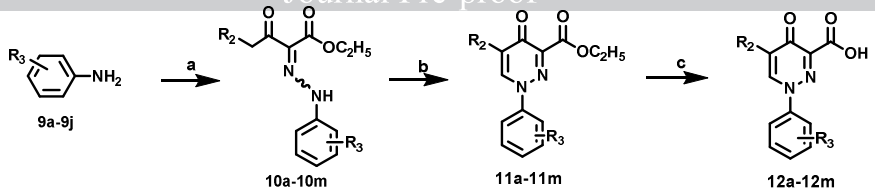

9a:R_3=2-CF_3 9b:R_3=3-CF_3,4-Cl 9c:R_3=2-CH_3 9d:R_3=H 9e:R_3=2-F 9f:R_3=3-Cl,4-F

9g:R_3=2,4-2CH_3 9h:R_3=3-CF_3 9i:R_3=3-CH_3 9j:R_3=4-CH_3 10a,11a,12a:R_2=H,R_3=2-CF_3

10b,11b,12b:R_2=CH_3,R_3=3-CF_3,4-Cl 10c,11c,12c:,R_2=CH_3,R_3=2-CH_3 10d,11d,12d:R_2=H,R_3=2-CH_3 10e,11e,12e:R_2=CH_3,R_3=2-F

10f,11f,12f:R_2=CH_3,R_3=H 10g,11g,12g:R_2=CH_3,R_3=3-Cl,4-F 10h,11h,12h:R_2=CH_3,R_3=2,4-2CH_3 10i,11i,12i:R_2=CH_3,R_3=3-CH_3

10j,11j,12j:R_2=CH_3,R_3=4-CH_3 10k,11k,12k:R_2=H,R_3=H 10l,11l,12l:R_2=CH_3,R_3=3-CF_3 10m,11m,12m:R_2=CH_2CH_3,R_3=H

Scheme 3. Preparation of intermediates **12a-12m.** Reagents and conditions: (a) i: conc HCl, $NaNO_2$, H_2O, 0 °C,0.5 h; ii: different ethyl acyl acetate, AcONa, H_2O/EtOH, rt, 5-8 h; (b) DMF-DMA, toluene, 110 °C, 5-8 h; (c) NaOH, H_2O, 40°C, 2-5 h;

2.3. Biological evaluation

2.3.1. HDAC1 and c-Met enzymatic activity assay

Initially, the abilities of compounds **14a-14y** to inhibit HDAC1 and c-Met were preliminarily screened at 100 nM concentration, respectively, with SAHA, Cabozantinib and AC-386 as the positive controls.

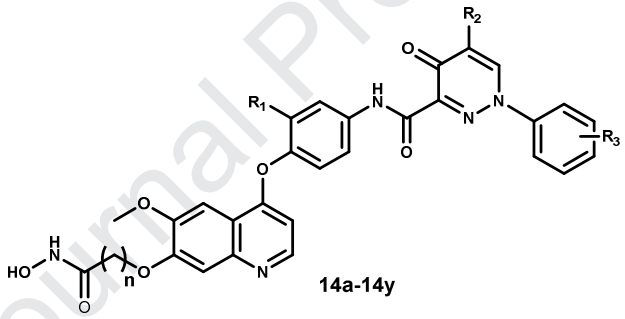

Table 1. HDAC1 and c-Met inhibitory activities of target compounds **14a-14y**

Compd.	n	R_1	R_2	R_3	HDAC1inhibition @ 100nM[a]	c-Met inhibition @ 100nM[a]
14a	1	H	H	2-CF_3	1.2%	56.3%
14b	1	H	CH_3	3-CF_3,4-Cl	5.2%	50.2%
14c	1	H	CH_3	2-CH_3	NI[b]	63.5%
14d	3	F	CH_3	2-CH_3	8.0%	95.5%
14e	3	F	CH_3	H	2.5%	98.3%
14f	3	F	H	2-CH_3	6.0%	93.5%
14g	3	F	CH_3	2-F	7.1%	94.0%

14h	3	H	CH_3	2-F	9.2%	90.8%
14i	3	H	CH_3	2-CH_3	10.7%	98.5%
14j	3	H	H	H	12.6%	96.4%
14k	5	F	CH_3	2-F	61.1%	89.1%
14l	5	F	CH_3	H	53.3%	95.0%
14m	5	H	H	2-CH_3	62.1%	90.4%
14n	5	H	CH_3	2-CH_3	36.9%	95.7%
14o	6	H	CH_3	H	86.6%	88.6%
14p	6	H	CH_3	2-CH_3	89.1%	78.6%
14q	6	H	CH_3	3-Cl,4-F	40.0%	61.1%
14r	6	H	CH_3	2,4-$(CH_3)_2$	65.3%	63.8%
14s	6	H	CH_3	3-CF_3	35.3%	46.3%
14t	6	F	CH_3	2-CH_3	53.0%	63.1%
14u	6	F	H	2-CH_3	59.5%	76.7%
14v	6	H	CH_3	3-CH_3	62.0%	76.5%
14w	6	H	CH_3	4-CH_3	47.6%	72.8%
14x	**6**	**H**	**H**	**H**	**88.0**%	**96.3**%
14y	6	H	CH_2CH_3	H	86.4%	78.2%
SAHA[c]					88.4%	2.80%
XL-184[c]					–	93.1%
AC-386[c]					—	93.8%

[a] All compounds were assayed at least twice, and the inhibitory values were averaged.

[b] NI = no inhibition.

[c] Used as a positive control.

The biological data listed in **Table 1** showed that all compounds showed similar or superior c-Met inhibitory

activities even compared with the positive controls, however only half of the compounds inhibited HDAC1 over 50% rate at 100 nM. The SARs on the length of the linker were firstly studied. Compounds **14a**, **14b** and **14c** with a one-carbon linker did not show any appreciable inhibition against HDAC1 (inhibition rates ranging from 0 % to 5.2%). As the length of the linker was increased to three carbons, a weak HDAC1 potency was still observed. However, the c-Met activity was enhanced about 1.5-fold (**14c**: inhibition rate 63.5 % *vs* **14i**: inhibition rate 98.5%). As the linker length increased further (e.g., **14k** and **14l**), HDAC1 potency was boosted by over 20-fold (e.g., **14l** vs **14e**). Of particular note, compounds with six-carbon linker exhibited notable HDAC1 potency (e.g., **14o**, **14p** and **14x**), comparable to that of the launched HDAC inhibitors (e.g., SAHA). This study clearly showed that the linker length is highly important for HDAC1 activity, probably because the short linker could not lead their hydroxamate groups to the zinc ion to form an effective interaction. These results also suggested that six carbon atoms chain of the linker region was the optimal group to maintain the inhibitory activities for HDAC1. Interestingly, the linker length had no significant influence on c-Met inhibition of these dual inhibitors. (e.g., **14i**: inhibition rate 98.5%; **14n**: inhibition rate 95.7%; **14p**: inhibition rate 78.6%).

Further studies were performed to determine how R_1 affects activity. Compound **14i** with a H atom on the phenyl ring exhibited better activity than **14d** with a fluorine atom. The increase in activity can also be observed by comparing compounds **14p** (HDAC1: inhibition rate 89.1 %; c-Met: inhibition rate 78.6%) with **14t** (HDAC1: inhibition rate 53.0 %; c-Met: inhibition rate 63.1%).

Additional investigations were performed to study the effect of different substituents on the phenyl ring on the enzymatic activity. Introduction of electron-withdrawing groups on the phenyl ring led to a slightly loss in c-Met inhibitory activity as compared with compounds with electron-donating groups (**14c** *vs* **14b**; **14i** *vs* **14h**). Once we identified suitable substituents, we then investigate which position affects activity, the results showed that the ortho-substitution is better than the meta and the para-substitution of the phenyl ring (**14p** *vs* **14v** *vs* **14w**).

The last investigation was performed by introducing different R_2 to the dihydropyridazine ring to explore whether the size of R_2 group was closely related to antitumor activity. However, the introduction of methyl or ethyl group can not lead to an obvious improvement in activity (e.g., **14x**：HDAC1: inhibition rate 88.0 %; c-Met: inhibition rate 96.3%; **14o**: HDAC1: inhibition rate 86.6 %; c-Met: inhibition rate 88.6%; **14y**: HDAC1: inhibition rate 86.4 %; c-Met: inhibition rate 78.2%).

Considering the potent activity of compounds **14o**, **14x** and **14y** in inhibition of c-Met and HDAC1, the IC_{50} values were determined. As showed in **Table 2**, the tested compounds exhibited excellent c-Met enzymatic potency with IC_{50} values ranging from 5.40 to 19.86 nM and moderate HDAC1 enzymatic potency with IC_{50}

values ranging from 18.49 to 34.84 nM. In particular, compound **14x** showed the most potent activity against HDAC1 with an IC_{50} of 18.49 nM, which was comparable to that of SAHA (IC_{50} = 14.15 nM). However, the potency of **14x** against c-Met (IC_{50} = 5.40 nM) was slightly superior to AC-386 (IC_{50} = 7.42 nM), and was 6.9-fold higher than that of XL184 (IC_{50} = 37.28 nM).

Table 2. Enzymatic assays for HDAC1/c-Met inhibition.

Compd.	HDAC1 IC_{50} (nM) ± SD[a]	c-Met IC_{50} (nM) ± SD[a]
14o	34.03 ± 0.22	19.86 ± 0.10
14x	18.49 ± 0.18	5.40 ± 0.05
14y	34.84 ± 0.36	14.23 ± 0.15
SAHA[b]	14.15 ± 0.25	NT
XL-184[b]	NT	37.28 ± 1.10
AC-386[b]	NT	7.42 ± 0.20

[a] SD: standard deviation.

[b] Positive control.

NT= not tested.

2.3.2. In vitro cytotoxic activities

After the synthesis and evaluation for enzymatic activity assays of these compounds, antiproliferative effects of these compounds against HCT-116 (human colon cancer), A549 (human lung adenocarcinoma) and MCF-7 (human breast cancer) cell lines were tested using MTT assay.

Table 3. The antiproliferative activities of **14a-14y** against HCT-116, MCF-7and A549 cell lines in vitro.

Compd.	n	R_1	R_2	R_3	IC_{50} [a] (μmol/L) ± SD		
					HCT-116	MCF-7	A549
14a	1	H	H	2-CF_3	9.50 ± 0.40	6.32 ± 0.41	>20
14b	1	H	CH_3	3-CF_3,4-Cl	0.35 ± 0.03	3.48 ± 0.20	1.59 ± 0.31
14c	1	H	CH_3	2-CH_3	9.26 ± 1.01	8.78 ± 2.13	5.98 ± 0.10
14d	3	F	CH_3	2-CH_3	2.04 ± 0.03	2.60 ± 0.12	2.09 ± 0.30
14e	3	F	CH_3	H	0.66 ± 0.15	1.90 ± 0.23	1.90 ± 0.11

14f	3	F	H	2-CH_3	3.98 ± 0.07	3.20 ± 0.14	5.74 ± 0.61
14g	3	F	CH_3	2-F	1.12 ± 0.05	2.10 ± 0.17	1.37 ± 0.02
14h	3	H	CH_3	2-F	0.95 ± 0.08	2.65 ± 0.21	3.92 ± 0.36
14i	3	H	CH_3	2-CH_3	0.64 ± 0.03	1.60 ± 0.01	4.46 ± 0.51
14j	3	H	H	H	0.94 ± 0.04	7.41 ± 1.10	9.26 ± 0.46
14k	5	F	CH_3	2-F	0.59 ± 0.02	2.32 ± 0.04	1.32 ± 0.50
14l	5	F	CH_3	H	0.69 ± 0.14	2.33 ± 0.10	4.17 ± 0.09
14m	5	H	H	2-CH_3	0.70 ± 0.02	4.36 ± 0.50	3.92 ± 0.17
14n	5	H	CH_3	2-CH_3	0.29 ± 0.03	1.83 ± 0.06	1.82 ± 0.21
14o	6	H	CH_3	H	0.15 ± 0.02	1.61 ± 0.10	0.42 ± 0.04
14p	6	H	CH_3	2-CH_3	0.66 ± 0.05	1.83 ± 0.22	3.13 ± 0.37
14q	6	H	CH_3	3-Cl,4-F	0.37 ± 0.06	2.20 ± 0.10	0.38 ± 0.04
14r	6	H	CH_3	2,4-$(CH_3)_2$	0.44 ± 0.06	2.43 ± 0.21	1.84± 0.33
14s	6	H	CH_3	3-CF_3	0.59 ± 0.02	0.75 ± 0.11	0.78 ± 0.05
14t	6	F	CH_3	2-CH_3	2.30 ± 0.41	2.69 ± 0.11	4.28 ± 0.32
14u	6	F	H	2-CH_3	4.39 ± 0.89	3.65 ± 0.15	>20
14v	6	H	CH_3	3-CH_3	0.37 ± 0.03	1.68 ± 0.10	0.28 ± 0.09
14w	6	H	CH_3	4-CH_3	0.40 ± 0.02	2.56 ± 0.15	0.16 ± 0.04
14x	**6**	**H**	**H**	**H**	**0.22 ± 0.09**	**1.59 ± 0.06**	**0.22 ± 0.04**
14y	6	H	CH_2CH_3	H	0.30 ± 0.01	1.21 ± 0.22	0.23 ± 0.03
SAHA[b]					0.55 ± 0.13	2.00 ± 0.20	1.70 ± 0.12
XL-184[b]					4.67 ± 0.05	5.98 ± 0.15	7.80 ± 0.40
AC-386[b]					0.37± 0.02	0.63 ± 0.05	1.12 ± 0.10

[a] Inhibition values represent the average of at least three independent experiments.

[b] Used as a positive control.

Data in **Table 3** illustrated that the target compounds **14a-14y** exhibited moderate to potent antiproliferation

activities against one or more tested cancer cells with potencies in the single digit micromole range, which were mostly in accordance with the trend in enzymatic activity. Similarly, a clear dependency of the potency on the linker length is present, where the antiproliferative potency initially increased with the elongation of the linker. Compounds **14o**, **14s**, **14v**, **14x** and **14y** with six carbon linkers were the more potent compounds. Interestingly, most of the compounds were more potent against HCT-116 cell line than the other two cancer cell lines (MCF-7 and A549), indicating that the target compounds might be used in treating human colon cancer. Among them, compound **14x** exhibited the best activity against all of the tested cell lines with IC_{50} values of 0.22 μM, 1.59 μM and 0.22 μM against HCT-116, MCF-7 and A549 cell lines respectively.

We further examined the HCT-116, MCF-7 and A549 cell lines with a phase-contrast light microscope for changes in cell morphology in response to 72 h treatment with 0.5 μM, 1.0 μM and 4.0 μM **14x** (**Fig.4**). Through electronic microscope, some cells appear to be rounded, formation of membrane bubbles and apoptotic bodies. To our surprise, **14x** did not only affect cell morphology but also strongly inhibits cell proliferation even at the concentration of 0.5 μM. Because compound 1**4x** showed the highest potency in inhibition of both cell proliferation and c-Met/HDAC enzyme, it was advanced for further evaluation.

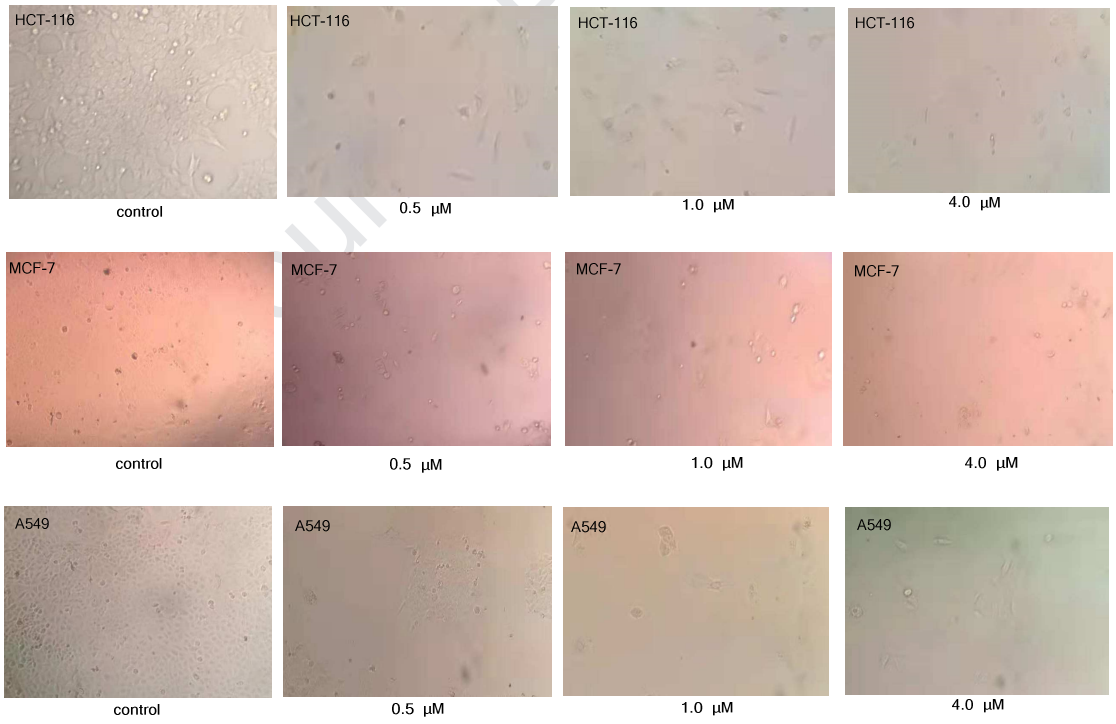

Fig.4. HCT-116, MCF-7 and A549 cell states after treatment with vehicle,0.5 μM, 1.0 μM L and 4.0 μM **14x** for 72h. Figures are representative of n ≥ 3 experiments.

2.3.3. Cell apoptosis study

In addition, we wanted to understand the mechanism of cell death, **14x** was selected for apoptosis study in HCT-116 cells using annexin V-FITC and PI staining and analyzed by flow cytometry (**Fig. 5**). After treating HCT-116 cells with 0.2 μM, 1.0 μM and 5.0 μM of **14x** for 48 h, the percentage of apoptotic cells was 4.19%, 11.53% and 21.48%, respectively, which displayed a higher apoptosis level than control (3.48%). It was evident that **14x** is effective in the induction of cancer cell apoptosis in a dose-dependent manner.

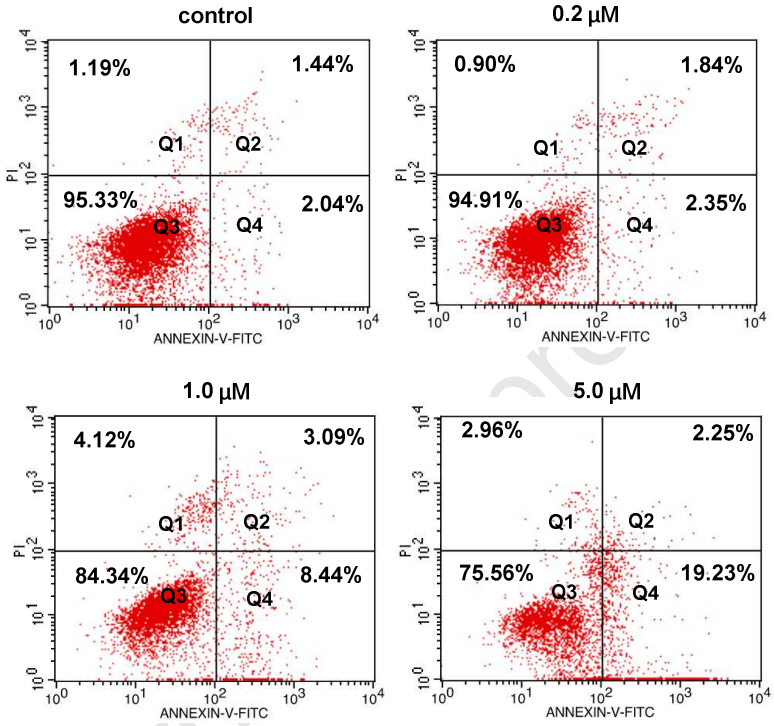

Fig. 5. Compound **14x** induced apoptosis in HCT-116 cells. Cells were treated with various concentrations of **14x** for 48 h and then analyzed the Annexin V-FITC/PI staining test by flow cytometry analysis. Values represent the mean ± S.D, n = 3. The percentage of cells in each part is indicated.

2.3.4. Cell cycle analysis

To probe the effect of compound **14x** on various phases of cell cycle progression，flow cytometry experiment was performed on HCT-116 cells. After treatment of HCT-116 cells with **14x** for 48 h at indicated concentrations (0.2 μM, 1.0 μM, 5.0 μM), the cells were fixed and stained with PI, the DNA content was evaluated by flow cytometric method. The obtained results were compared with non-treated HCT-116 cells as control. As shown in **Fig. 6-7**, it was clearly observed that the percentage of cells in G2/M-phase for compound **14x** was increased from 11.74% (control group) to 14.59%, 80.03%, and 81.22%. These results confirmed that compound **14x** significantly caused G2/M-phase arrest in HCT-116 cells in a dose dependent manner.

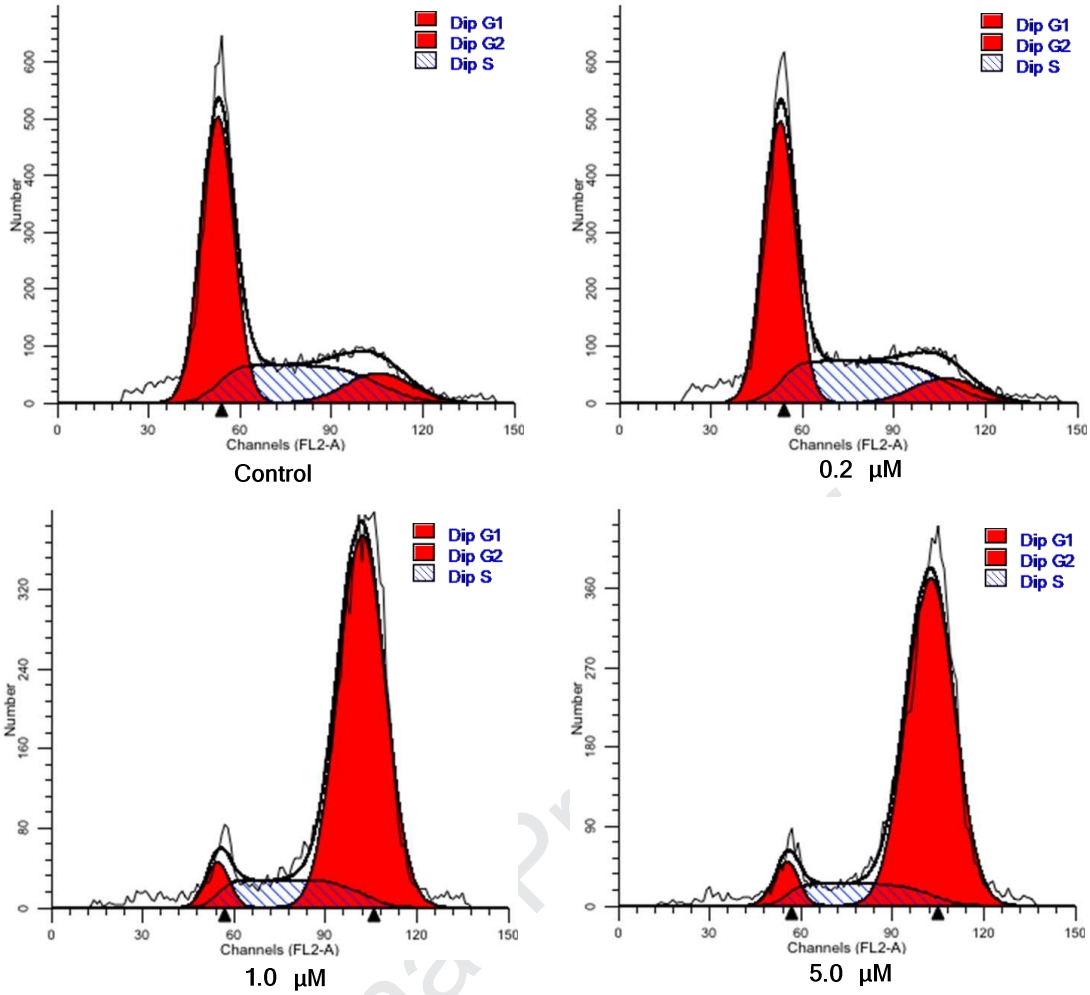

Fig. 6. Effect of compound **14x** on the cell cycle distribution of HCT-116 cells. The experiments were performed three times and a representative experiment is shown.

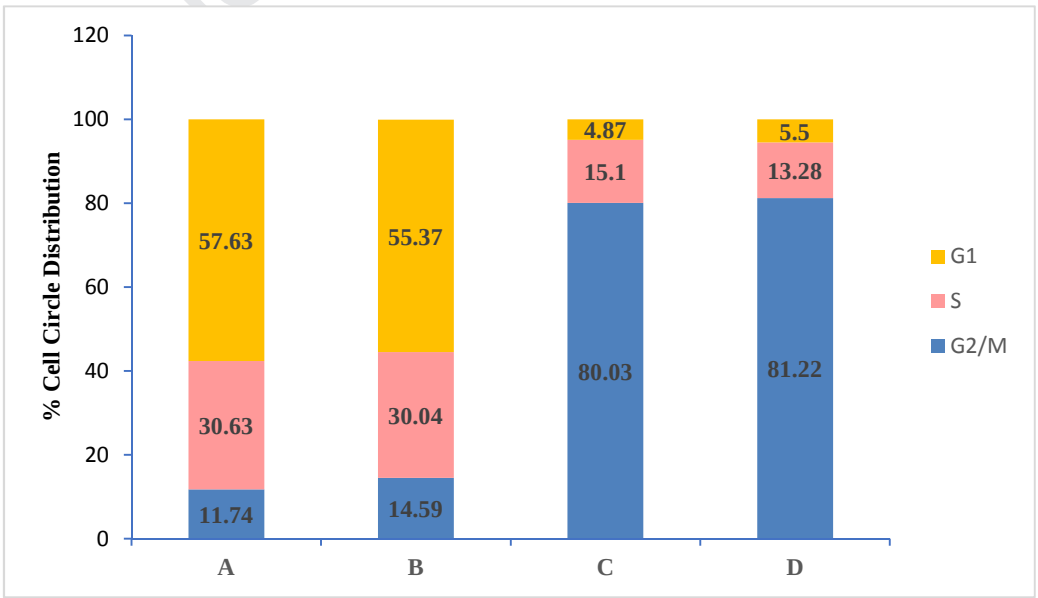

Fig. 7. Quantitative analysis of cell cycle distributions; (**A**) Non-treated cells as control group; (**B**) treated with **14x** at 0.2 µM; (**C**)

treated with **14x** at 1.0 μM; (**D**) treated with **14x** at 5.0 μM.

2.3.5. Binding Mode of the c-Met/HDAC Dual Inhibitors.

To investigate the binding mode of compound **14x** with c-Met and HDAC1, molecular docking studies were performed [23,31]. As shown in **Fig. 8: A, B** (PDB ID: 3LQ8), the quinoline scaffold fits well into the c-Met ATP binding pocket and forms a hydrogen bond with the residue of Met1160. The H atom of the amide and the N atom of pyridazinone scaffold of compound **14x** formed two hydrogen bonds with Asp1222. In addition, the carbonyl of pyridazinone formed hydrogen bond with Lys1110. These interactions were identified as the key driving force for the c-Met binding. It was also revealed that the hydroxamic tail formed two hydrogen bonds with residues of His1162 and Asn1171, which resulted in the improvement of c-Met activity comparing to the hit AC-386. Compound **14x** bound with HDAC1 (PDB ID:1C3S), mainly through ZBG (**Fig. 8: C, D**). The hydroxamic acid of **14x** coordinated to the catalytic Zn^{2+} of HDAC1 and formed hydrogen bond with His170.

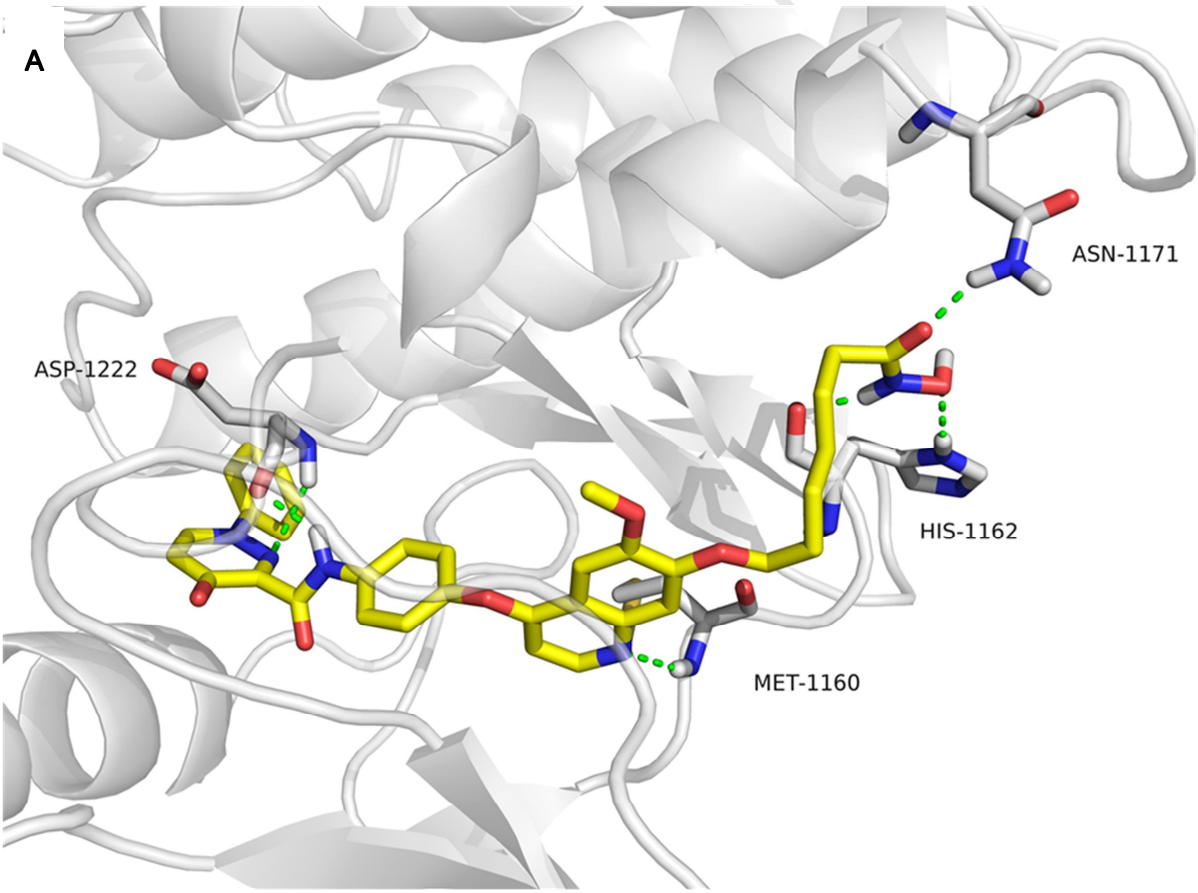

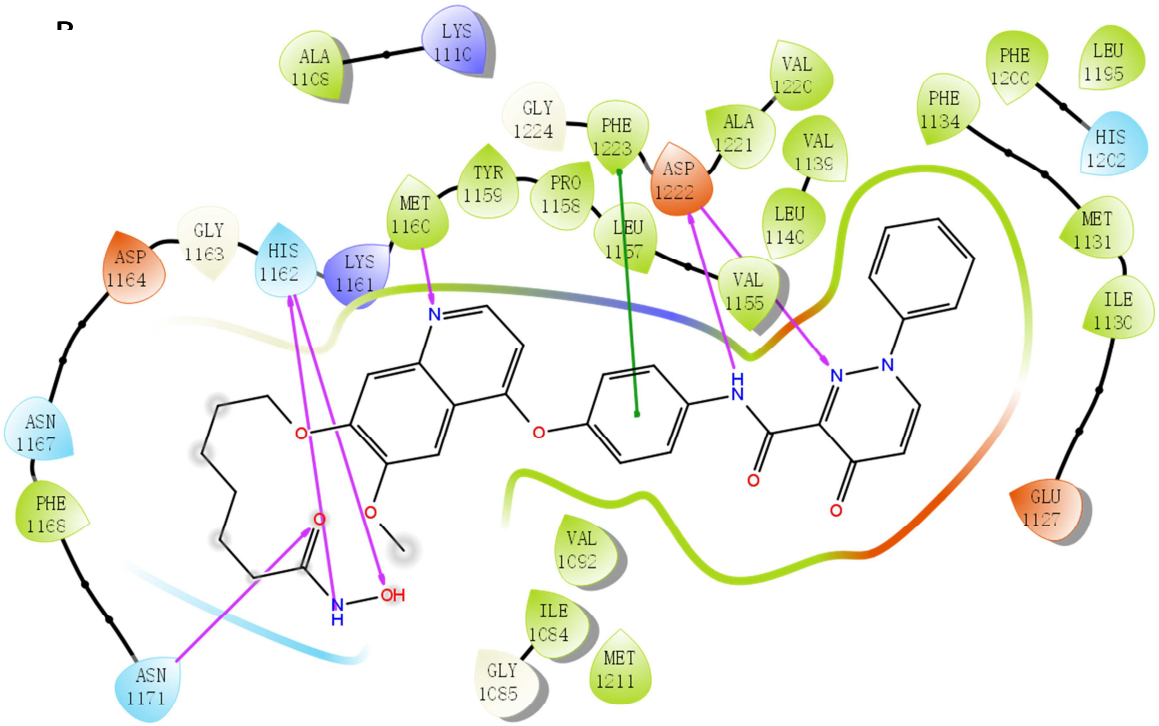
LYS 1110
ALA 1108
GLY 1224
PHE 1223
ASP 1222
ALA 1221
VAL 1220
PHE 1200
LEU 1195
PHE 1134
HIS 1202
VAL 1139
LEU 1140
MET 1131
ILE 1130
GLU 1127
TYR 1159
PRO 1158
MET 1160
LEU 1157
VAL 1155
GLY 1163
HIS 1162
LYS 1161
ASP 1164
ASN 1167
PHE 1168
ASN 1171
VAL 1092
ILE 1084
GLY 1085
MET 1211
Charged (negative)
Charged (positive)
Glycine
Hydrophobic
Metal
Polar
Unspecified residue
Water
Hydration site
Hydration site (displaced)
Distance
H-bond
Metal coordination
Pi-Pi stacking
Pi-cation
Salt bridge
Solvent exposure

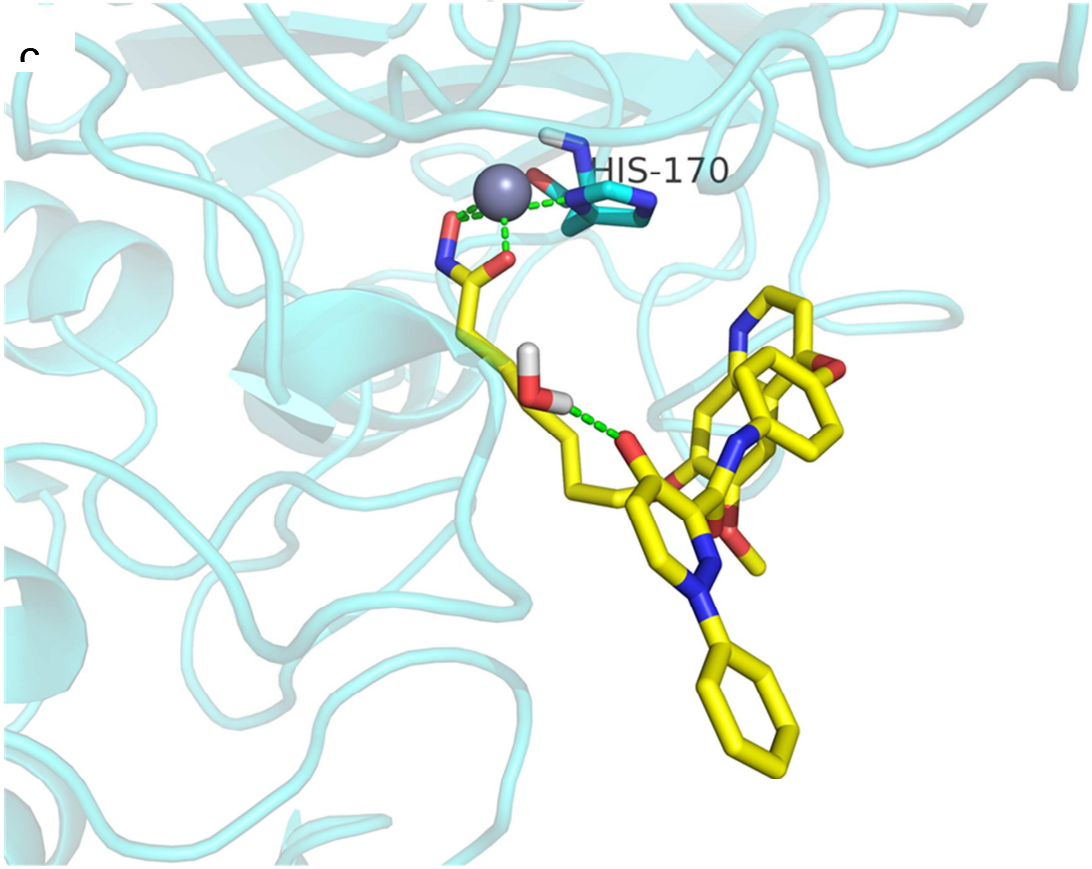
HIS-170

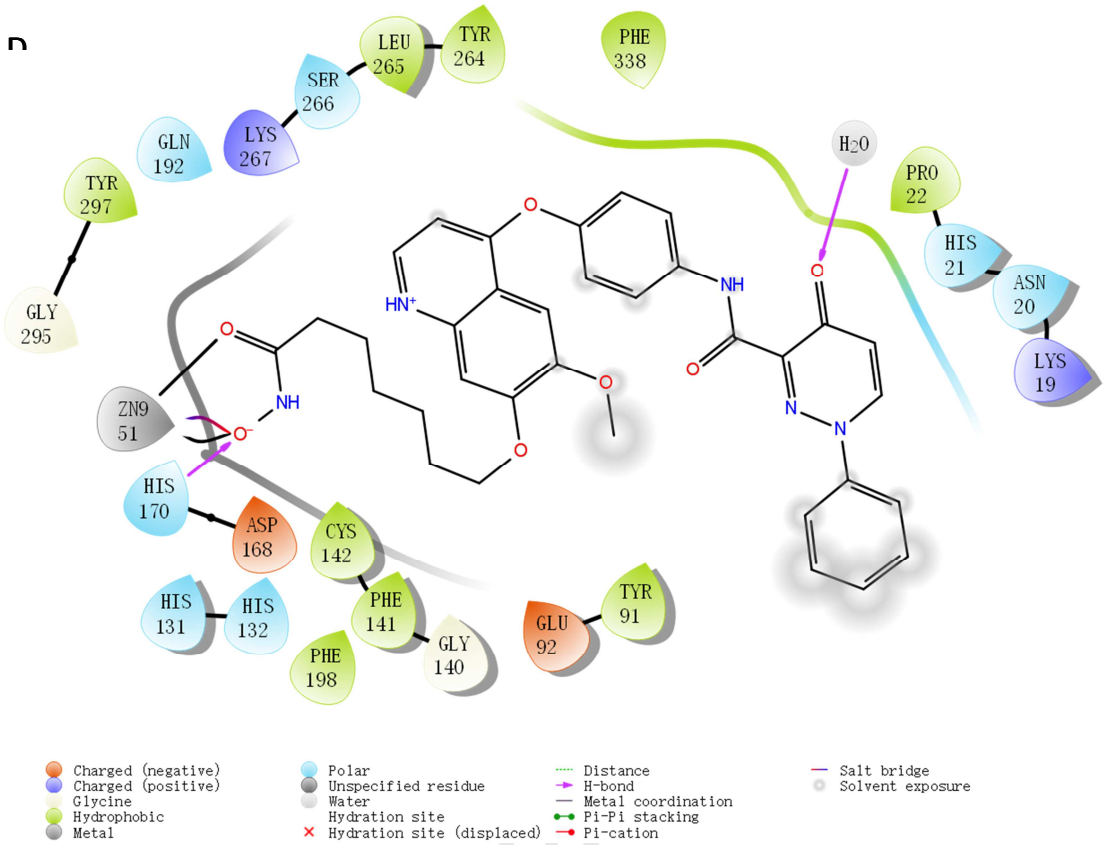

Fig. 8. (A) Proposed 3D binding mode of compound **14x** in the active site of c-Met (PDB: 3LQ8). **(B)** Proposed 2D binding mode of compound **14x** in the active site of c-Met (PDB: 3LQ8). (**C**) Proposed 3D binding mode of compound **14x** in the active site of HDAC1 (PDB: 1C3S). (**D**) Proposed 2D binding mode of compound **14x** in the active site of HDAC1 (PDB: 1C3S). The figure was generated using PyMol (http://www.pymol.org/).

3. Conclusions

In conclusion, on the basis of structural information for HDAC as well as the available structure-activity relationship data of our previous c-Met inhibitor AC-386, we designed a novel chemical series of dual inhibitors simutaneously targeting c-Met and HDAC. In biochemical assays, most of analogues showed potent inhibition of c-Met and HDAC1 enzymatic activity. In addition, the SAR analyses around the linker and substituents led us to find a lead molecule **14x**. The results of antiproliferative activity indicated that **14x** significantly exhibited inhibitory activity against HCT-116, MCF-7 and A549 cell lines. Cell apoptosis study found **14x** was highly effective in the induction of apoptosis in a dose-dependent manner. Cell cycle analysis of **14x** by flow cytometry showed cell cycle arrest in G2/M phase. Compound **14x** could bind well with active sites of c-Met and HDAC1 in molecular docking study. Overall, **14x** was a potential lead compound for cancer therapy. Extensive investigations of the pharmacokinetics and *in vivo* activity of **14x** are ongoing in our lab and the results will be reported in due course.

4. Experimental

4.1 Chemistry

Unless otherwise specified, all materials were obtained from commercial suppliers and were used without further purification. Reactions' time and purity of the products were monitored by TLC on FLUKA silica gel aluminum cards (0.2 mm thickness) with fluorescent indicator 254 nm. Column chromatography was run on silica gel (200–300 mesh) from Qingdao Ocean Chemicals (Qingdao, Shandong, China). All melting points were obtained on a Büchi Melting Point B-540 apparatus (Büchi Labortechnik, Flawil, Switzerland) and were uncorrected. Mass spectra (MS) were taken in ESI mode on Agilent 1100 LC–MS (Agilent, Palo Alto, CA, USA). The reverse phase HPLC was conducted on an Agilent 1260 Infinity chromatograph, which was equipped with ZORBAX SB-C18 column (250 mm × 4.6 mm). The mobile phase A was methanol, and mobile phase B was 30 mM NaH_2PO_4 in water (pH 2.5). The gradient of 5−95% A was run at a flow rate of 1.0 mL/min over 30 min. High-resolution mass spectra (HRMS) were measured with an Agilent Accurate-Mass Q-TOF 6530 in ESI mode (Agilent, Santa Clara, CA, USA). ^{1}HNMR and ^{13}C NMR spectra were performed using Bruker spectrometers (BrukerBioscience, respectively, Billerica, MA, USA) with TMS as an internal standard.

*4.1.1 Preparation of ethyl 2-((4-(4-aminophenoxy)-6-methoxyquinolin-7-yl)oxy)acetate (**8a**) [29]*

*4.1.1.1 Preparation of ethyl 2-(4-acetyl-2-methoxyphenoxy)acetate (**2a**)*

To a solution of 4-hydroxy-3-methoxy-acetophenone (20.0 g, 120.5 mmol) in DMF (200 mL) was added K_2CO_3 (17.4 g, 126.5 mmol) and ethyl 2-bromoacetate (20.9 g, 126.5 mmol). The reaction mixture was then stirred at 80 °C for 3 h. The mixture was then poured into cold water (500 mL) with vigorously agitating, and the resulting precipitate was filtered-off, washed with water, and dried under vacuum to afford the title compound **2a** (27.5 g, 90.5%) as a white solid. MS (ESI) m/z: 253.15 $[M+H]^+$.

*4.1.1.2 Preparation of ethyl 2-(4-acetyl-2-methoxy-5-nitrophenoxy)acetate (**3a**)*

A stirred solution of **2a** (25.0 g, 99.2 mmol) in CH_2Cl_2 (250 mL) was cooled to 10 °C, fuming HNO_3 (46.8 g, 495.8 mmol) was added at an appropriate rate keeping the temperature below -5 °C. The reaction mixture was allowed to stir at -5 °C for 6 h, then poured into cold water (200 mL), the organic layer was separated and washed with water (200 mL), then concentrated under reduced pressure to afford crude **3a** as a light yellow solid (24.3 g, 82.5%). MS (ESI) m/z: 298.13 $[M+H]^+$.

*4.1.1.3 Preparation of ethyl (E)-2-(4-(3-(dimethylamino)acryloyl)-2-methoxy-5-nitrophenoxy)acetate (**4a**)*

20.0 g (67.3 mmol) of **3a** was suspended in 200 mL of toluene at room temperature, then DMF-DMA (24.0 g, 202.0 mmol) was added to a solution. The reaction was heated to 110°C until TLC showed the completion of the reaction. After cooling to rt, the resultant solid was collected by filtration, washed with toluene (30 mL), and then dried under vacuum to yield **4a** as a yellow solid (14.4 g, 60.8%). MS (ESI) m/z: 353.23 $[M+H]^+$.

*4.1.1.4 Preparation of ethyl 2-((6-methoxy-4-oxo-1,4-dihydroquinolin-7-yl)oxy)acetate (**5a**)*

Fe powder (11.1 g, 199.0 mmol) was added to a solution of **4a** (14.0 g, 39.8 mmol) in acetic acid (70 mL) at 60 °C in batches, then the mixture was stirred at 80 °C for 2 h. The hot solution was filtered through celite and washed with hot acetic acid. The combined filtrate was cooled to rt, the resultant solid was collected by filtration and washed with acetic acid (10 mL) to afford **5a** as a pale solid (7.2 g, 65.0%). MS (ESI) m/z: 278.33 $[M+H]^+$.

*4..1.1.5 Preparation of ethyl 2-((4-chloro-6-methoxyquinolin-7-yl)oxy)acetate (**6a**)*

A mixture consisting of 7.0 g (25.3 mmol) of **5a** and 56.0 mL (8 v/m) of phosphorus oxychloride was refluxed for 8 h whereby a clear solution was formed. Thereafter, the excess unreacted phosphorus oxychloride was evaporated in vacuo and the residual oil was poured into ice water. The precipitate formed under vigorous stirring conditions, thereby was collected by vacuum filtration, dried under reduced pressure to afford product **6a** as a white solid (6.3 g, 83.7%). MS (ESI) m/z: 296.10 $[M+H]^+$.

*4.1.1.6 Preparation of ethyl 2-((6-methoxy-4-(4-nitrophenoxy)quinolin-7-yl)oxy)acetate (**7a**)*

4-nitrophenol (4.2 g 30.5 mmol) was added to a stirred solution of **6a** (6.0 g, 20.3 mmol) in 60 mL chlorobenzene, then the reaction mixture was refluxed for 25 h whereby a clear solution was formed. Then evaporated in vacuo, the resulting precipitate was added to 100 mL DCM, the organic portion was washed with 10% w/w aqueous sodium bicarbonate solution (3 x 50 mL), the organic layer was evaporated in vacuo and dried under reduced pressure to afford product **7a** as a pale solid (4.8 g, 60.4%). MS (ESI) m/z: 399.18 $[M+H]^+$.

*4.1.1.7 Preparation of ethyl 2-((4-(4-aminophenoxy)-6-methoxyquinolin-7-yl)oxy)acetate (**8a**)*

10% Pd/C (0.45 g, 10%w/w) was added to a stirred solution of **7a** (4.5 g, 11.3 mmol) in 45 mL methanol under H_2, then the mixture was stirred at 40 °C for 4 h. After completion of reaction, it was allowed to cool to room temperature. The solution was filtered through celite and washed with methanol (10 mL), then solvent was evaporated in vacuo and dried under reduced pressure to afford product **8a** as a rubricans solid. (4.0 g, 96.2%). MS (ESI) m/z (%): 369.32 $[M+H]^+$.

The preparation of the key intermediates **8b-8g** are the same way as to preparation **8a**, So the synthesis method would not be listed here.

*4.1.2 Preparation of ethyl 4-((4-(4-aminophenoxy)-6-methoxyquinolin-7-yl)oxy)butanoate (**8b**)*

Pale solid; total yield: 12.7%; MS (ESI) m/z (%): 397.22 $[M+H]^+$.

*4.1.3 Preparation of ethyl 4-((4-(4-amino-2-fluorophenoxy)-6-methoxyquinolin-7-yl)oxy)butanoate (**8c**)*

Black solid; total yield: 10.5%; MS (ESI) m/z (%): 415.21 $[M+H]^+$.

*4.1.4 Preparation of ethyl 6-((4-(4-aminophenoxy)-6-methoxyquinolin-7-yl)oxy)hexanoate (**8d**)*

Black solid; total yield: 9.8%; MS (ESI) m/z (%): 425.33 $[M+H]^+$.

*4.1.5 Preparation of ethyl 6-((4-(4-amino-2-fluorophenoxy)-6-methoxyquinolin-7-yl)oxy)hexanoate (**8e**)*

Black solid; total yield: 12.8%; MS (ESI) m/z (%): 443.42 $[M+H]^+$.

4.1.6 Preparation of ethyl 7-((4-(4-aminophenoxy)-6-methoxyquinolin-7-yl)oxy)heptanoate *(**8f**)*

Black solid; total yield: 14.1%; MS (ESI) m/z (%): 439.38 $[M+H]^+$. ^{1}H NMR (600 MHz, DMSO-d_6) δ 8.42 (d, J = 5.3 Hz, 1H), 7.50 (s, 1H), 7.34 (s, 1H), 6.93 (d, J = 8.7 Hz, 2H), 6.67 (d, J = 8.8 Hz, 2H), 6.36 (d, J = 5.2 Hz, 1H), 5.18 (s, 2H), 4.12 (t, J = 6.5 Hz, 2H), 4.05 (q, J = 7.1 Hz, 2H), 3.93 (s, 3H), 2.30 (t, J = 7.4 Hz, 2H), 1.80 (p, J = 6.7 Hz, 2H), 1.57 (p, J = 7.4 Hz, 2H), 1.47 (p, J = 7.5 Hz, 2H), 1.37 (q, J = 8.1 Hz, 2H), 1.18 (t, J = 7.1 Hz, 3H).

*4.1.7 Preparation of ethyl 7-((4-(4-amino-2-fluorophenoxy)-6-methoxyquinolin-7-yl)oxy)heptanoate (**8g**)*

Black solid; total yield: 15.1%; MS (ESI) m/z (%): 457.35 $[M+H]^+$.

*4.1.8 General procedure for preparation intermediates (**10a-10m**)*

To a mixture of substituted phenyl amine (60.0 mmol) and 6 M/L HCl (60 mL), $NaNO_2$ (5 g, 72.0 mmol) in H_2O (200 mL) was added dropwise at 0 ℃. After the completion of addition, the reaction mixture was stirred at 0 ℃ for 30 min, then added into a mixture of different ethyl acyl acetate (63.0 mmol), anhydrous sodium acetate (180.0 mmol) and EtOH (200 mL) at 0 ℃ and stirred for another 2 h. Then the mixture was filtered, and the residue was dried to afford light yellow solids **10a-10m** in 70-95% yields.

*4.1.8.1 Preparation of ethyl 3-oxo-2-(2-(2-(trifluoromethyl)phenyl)hydrazono)butanoate (**10a**)*

Yellow solid; yield: 74.1%; MS (ESI) m/z (%): 303.12 $[M+H]^+$.

*4.1.8.2 Preparation of ethyl 2-(2-(4-chloro-3-(trifluoromethyl)phenyl)hydrazono)-3-oxopentanoate (**10b**)*

Light yellow solid; yield: 79.8%; MS (ESI) m/z (%): 351. 25 $[M+H]^+$.

*4.1.8.3 Preparation of ethyl 3-oxo-2-(2-(o-tolyl)hydrazono)pentanoate (**10c**)*

Yellow solid; yield: 84.2%; MS (ESI) m/z (%): 263.20 $[M+H]^+$.

*4.1.8.4 Preparation of ethyl 3-oxo-2-(2-(o-tolyl)hydrazono)butanoate (**10d**)*

Yellow solid; yield: 88.1%; MS (ESI) m/z (%): 249.15 $[M+H]^+$.

*4.1.8.4 Preparation of ethyl 2-(2-(2-fluorophenyl)hydrazono)-3-oxopentanoate (**10e**)*

Yellow solid; yield: 95.0%; MS (ESI) m/z (%): 267.11 $[M+H]^+$.

*4.1.8.5 Preparation of ethyl 3-oxo-2-(2-phenylhydrazono)pentanoate (**10f**)*

Light yellow solid; yield: 70.1%; MS (ESI) m/z (%): 249.15 $[M+H]^+$.

*4.1.8.6 Preparation of ethyl 2-(2-(3-chloro-4-fluorophenyl)hydrazono)-3-oxopentanoate (**10g**)*

Yellow solid; total yield: 82.7%; MS (ESI) m/z (%): 301.11 $[M+H]^+$.

*4.1.8.7 Preparation of ethyl 2-(2-(2,4-dimethylphenyl)hydrazono)-3-oxopentanoate (**10h**)*

Light yellow solid; yield: 77.5%; MS (ESI) m/z (%): 277.18 $[M+H]^+$.

*4.1.8.8 Preparation of ethyl 3-oxo-2-(2-(m-tolyl)hydrazono)pentanoate (**10i**)*

Yellow solid; yield: 92.3%; MS (ESI) m/z (%): 263.15 $[M+H]^+$.

*4.1.8.9 Preparation of ethyl ethyl 3-oxo-2-(2-(p-tolyl)hydrazono)pentanoate (**10j**)*

Light yellow solid; yield: 90.6%; MS (ESI) m/z (%): 263.15 $[M+H]^+$.

*4.1.8.10 Preparation of ethyl 3-oxo-2-(2-phenylhydrazono)butanoate (**10k**)*

Yellow solid; yield: 79.5%; MS (ESI) m/z (%): 235.10 $[M+H]^+$.

*4.1.8.11 Preparation of ethyl 3-oxo-2-(2-(3-(trifluoromethyl)phenyl)hydrazono)pentanoate (**10l**)*

Light yellow solid; yield: 82.1%; MS (ESI) m/z (%): 317.19 $[M+H]^+$.

*4.1.8.12 Preparation of ethyl 3-oxo-2-(2-phenylhydrazono)hexanoate (**10m**)*

Light yellow solid; yield: 94.4%; MS (ESI) m/z (%): 263.15 $[M+H]^+$.

*4.1.9 General procedure for preparation intermediates (**11a-11m**)*

Appropriate intermediate **10a**-**10m** (20.0 mmol) was suspended in 50 mL of toluene at room temperature, then DMF-DMA (60.0 mmol) was added to a solution. The reaction was heated to 110 ℃ until TLC showed the completion of the reaction. After cooling to rt, the resultant solid was collected by filtration, washed with toluene (20 mL), and then dried under vacuum to yield **11a-11m** as yellow solids in 66-82% yields.

*4.1.9.1 Preparation of ethyl 4-oxo-1-(2-(trifluoromethyl)phenyl)-1,4-dihydropyridazine-3-carboxylate (**11a**)*

Yellow solid; yield: 84.0%; MS (ESI) m/z (%): 313.10 $[M+H]^+$.

*4.1.9.2 Preparation of ethyl 1-(4-chloro-3-(trifluoromethyl)phenyl)-5-methyl-4-oxo-1,4-dihydropyridazine-3-carboxylate (**11b**)*

Yellow solid; yield: 79.7%; MS (ESI) m/z (%): 361.15 $[M+H]^+$.

*4.1.9.3 Preparation of ethyl 5-methyl-4-oxo-1-(o-tolyl)-1,4-dihydropyridazine-3-carboxylate (**11c**)*

Yellow solid; yield: 74.9%; MS (ESI) m/z (%): 273.19 $[M+H]^+$.

*4.1.9.4 Preparation of ethyl 4-oxo-1-(o-tolyl)-1,4-dihydropyridazine-3-carboxylate (**11d**)*

Yellow solid; yield: 78.4%; MS (ESI) m/z (%): 259.22 $[M+H]^+$.

*4.1.9.5 Preparation of ethyl 1-(2-fluorophenyl)-5-methyl-4-oxo-1,4-dihydropyridazine-3-carboxylate (**11e**)*

Yellow solid; yield: 65.9%; MS (ESI) m/z (%): 277.19 $[M+H]^+$.

*4.1.9.6 Preparation of ethyl 5-methyl-4-oxo-1-phenyl-1,4-dihydropyridazine-3-carboxylate (**11f**)*

Yellow solid; yield: 74.6%; MS (ESI) m/z (%): 259.22 $[M+H]^+$.

*4.1.9.7 Preparation of ethyl 1-(3-chloro-4-fluorophenyl)-5-methyl-4-oxo-1,4-dihydropyridazine-3-carboxylate (**11g**)*

Yellow solid; total yield: 82.2%; MS (ESI) m/z (%): 311.10 $[M+H]^+$.

*4.1.9.8Preparation of ethyl 1-(2,4-dimethylphenyl)-5-methyl-4-oxo-1,4-dihydropyridazine-3-carboxylate (**11h**)*

Light yellow solid; yield: 70.1%; MS (ESI) m/z (%): 287.15 $[M+H]^+$.

*4.1.9.9 Preparation of ethyl 5-methyl-4-oxo-1-(m-tolyl)-1,4-dihydropyridazine-3-carboxylate (**11i**)*

Yellow solid; yield: 66.3%; MS (ESI) m/z (%): 273.19 $[M+H]^+$.

*4.1.9.10 Preparation of ethyl 5-methyl-4-oxo-1-(p-tolyl)-1,4-dihydropyridazine-3-carboxylate (**11j**)*

Yellow solid; yield:69.9%; MS (ESI) m/z (%): 273.19 $[M+H]^+$.

*4.1.9.11 Preparation of ethyl 4-oxo-1-phenyl-1,4-dihydropyridazine-3-carboxylate (**11k**)*

Yellow solid; yield: 79.3%; MS (ESI) m/z (%): 245.15 $[M+H]^+$.

*4.1.9.12 Preparation of ethyl 4-oxo-1-(3-(trifluoromethyl)phenyl)-1,4-dihydropyridazine-3-carboxylate (**11l**)*

Yellow solid; yield: 81.0%; MS (ESI) m/z (%): 327.32 $[M+H]^+$.

*4.1.9.13 Preparation of ethyl 5-ethyl-4-oxo-1-phenyl-1,4-dihydropyridazine-3-carboxylate (**11m**)*

Yellow solid; yield: 80.1%; MS (ESI) m/z (%): 273.19 $[M+H]^+$.

*4.1.10 General procedure for preparation intermediates (**12a-12m**)*

NaOH (100.0 mmol) was added to a stirred solution of intermediate **11a-11m** (20.0 mmol) in 40 mL H_2O, then the reaction mixture was heated at 40 °C for 2-5 h whereby a clear solution was formed. Then the reaction mixture was cool to room temperature, acidified (6 N HCl) to afford substituted acids (**12a-12m**) as white precipitates in 90-96% yields.

*4.1.10.1 Preparation of 4-oxo-1-(2-(trifluoromethyl)phenyl)-1,4-dihydropyridazine-3-carboxylic acid (**12a**)*

Yellow solid; yield: 94.2%, MS (ESI) m/z (%): 285.09 $[M-H]^-$;

*4.1.10.2 Preparation of 1-(4-chloro-3-(trifluoromethyl)phenyl)-5-methyl-4-oxo-1,4-dihydropyridazine-3-carboxylic acid (**12b**)*

White solid; yield: 91.7%, MS (ESI) m/z (%): 333.13 $[M+H]^+$;

*4.1.10.3 Preparation of 5-methyl-4-oxo-1-(o-tolyl)-1,4-dihydropyridazine-3-carboxylic acid (**12c**)*

White solid; yield: 94.9%, MS (ESI) m/z (%): 245.17 $[M+H]^+$;

*4.1.10.4 Preparation of 4-oxo-1-(o-tolyl)-1,4-dihydropyridazine-3-carboxylic acid (**12d**)*

White solid; yield: 90.2%, MS (ESI) m/z (%): 231.13 $[M+H]^+$;

*4.1.10.5 Preparation of 1-(2-fluorophenyl)-5-methyl-4-oxo-1,4-dihydropyridazine-3-carboxylic acid (**12e**)*

Yellow solid; yield: 92.4%, MS (ESI) m/z (%): 249.53 $[M+H]^+$; ^{1}H NMR (600 MHz, DMSO-d_6) δ 15.16 (s, 1H), 8.98 (dd, *J* = 1.8, 1.0 Hz, 1H), 7.77 (td, *J* = 7.9, 1.7 Hz, 1H), 7.70–7.63 (m, 1H), 7.58 (ddd, *J* = 10.8, 8.4, 1.3 Hz, 1H), 7.47 (td, *J* = 7.8, 1.3 Hz, 1H), 2.11 (d, *J* = 1.0 Hz, 3H).

*4.1.10.6 Preparation of 5-methyl-4-oxo-1-phenyl-1,4-dihydropyridazine-3-carboxylic acid (**12f**)*

Light yellow solid; yield: 96.5%, MS (ESI) m/z (%): 229.24 $[M-H]^-$;

*4.1.10.7 Preparation of 1-(3-chloro-4-fluorophenyl)-5-methyl-4-oxo-1,4-dihydropyridazine-3-carboxylic acid (**12g**)*

Yellow solid; total yield: 94.9%, MS (ESI) m/z (%): 283.13 $[M+H]^+$;

*4.1.10.8 Preparation of 1-(2,4-dimethylphenyl)-5-methyl-4-oxo-1,4-dihydropyridazine-3-carboxylic acid (**12h**)*

Light yellow solid; yield: 90.3%, MS (ESI) m/z (%): 259.21 $[M+H]^+$;

*4.1.10.9 Preparation of 5-methyl-4-oxo-1-(m-tolyl)-1,4-dihydropyridazine-3-carboxylic acid (**12i**)*

White solid; yield: 94.1%, MS (ESI) m/z (%): 245.17 $[M+H]^+$;

*4.1.10.10 Preparation of 5-methyl-4-oxo-1-(p-tolyl)-1,4-dihydropyridazine-3-carboxylic acid (**12j**)*

White solid; yield: 90.9%, MS (ESI) m/z (%): 245.23 $[M+H]^+$; ^{1}H NMR (600 MHz, DMSO-d_6) δ 15.57 (s, 1H), 9.23 (s, 1H), 7.70 (d, *J* = 8.4 Hz, 2H), 7.43 (d, *J* = 8.1 Hz, 2H), 2.40 (s, 3H), 2.15 (s, 3H).

*4.1.10.11 Preparation of 4-oxo-1-phenyl-1,4-dihydropyridazine-3-carboxylic acid (**12k**)*

White solid; yield: 95.3%, MS (ESI) m/z (%): 215.26 $[M-H]^-$; ^{1}H NMR (600 MHz, DMSO-d_6) δ 15.08 (s, 1H), 9.11 (d, *J* = 7.8 Hz, 1H), 7.78 (d, *J* = 7.3 Hz, 2H), 7.63 (t, *J* = 7.9 Hz, 2H), 7.54 (t, *J* = 7.4 Hz, 1H), 7.07 (d, *J* = 7.7 Hz, 1H).

*4.1.10.12 Preparation of 5-methyl-4-oxo-1-(3-(trifluoromethyl)phenyl)-1,4-dihydropyridazine-3-carboxylic acid (**12l**)*

White solid; yield: 91.0%, MS (ESI) m/z (%): 298.99 $[M+H]^+$;

*4.1.10.13 Preparation of 5-ethyl-4-oxo-1-phenyl-1,4-dihydropyridazine-3-carboxylic acid (**12m**)*

White solid; yield: 90.4%, MS (ESI) m/z (%): 245.56 $[M+H]^+$; ^{1}H NMR (600 MHz, DMSO-d_6) δ 15.48 (s, 1H), 9.09 (s, 1H), 7.82 (d, *J* = 7.4 Hz, 2H), 7.64 (t, *J* = 7.9 Hz, 2H), 7.56 (t, *J* = 7.4 Hz, 1H), 2.59 (q, *J* = 7.5 Hz, 2H), 1.20 (t, *J* = 7.5 Hz, 3H).

*4.1.11 General procedure for preparation of intermediates (**13a-13y**)*

A mixture of **8a-8g** (1.0 mmol) and different intermediates **12a-12m** (1.3 mmol), HATU (1.3 mmol) and TEA (1.3 mmol) in DCM (15 mL) was stirred at reflux for 3-5 h. After being cooled to rt, the mixture was washed successively with 10% aqueous potassium carbonate solution (20 mL×3) and brine (20 mL×2), the organic phase was dried over anhydrous sodium sulfate. The solid was removed by filtration, and the filtrate was concentrated to yield the **13a-13y** respectively, yeilds 70.3-82.5%. Without any purification, the intermediates were used for next procedure.

*4.1.12 General procedure for preparation of target compounds (**14a-14y**)*

A solution of sodium hydroxide (4.0 g, 100.0 mmol) in methanol (14 mL) was added to a stirred solution of hydroxylamine hydrochloride (4.7 g, 67.2 mmol) in methanol (24 mL) at 0 °C. The reaction mixture was stirred at 0 °C for 1 h. The precipitate was removed by filtration and the filtrate was collected to provide fresh hydroxylamine solution which was stored in a refrigerator before use. The appropriate esters **13a-13y** (1.0 mmol) was added to the above freshly prepared hydroxylamine solution (15 mL) at 0 °C, then NaOH (0.04 g,1.0 mmol) was added to the solution. The reaction mixture was stirred at room temperature for 2-6 h. The reaction mixture was neutralized with 6 N HCl. The formed precipitate was collected by filtration, washed with water, dried in vacuo and purified by silica gel chromatography to afford target compounds **14a-14y** *in* 41.2-87.5% yields.

4.1.12.1.

*N-(4-((7-(2-(hydroxyamino)-2-oxoethoxy)-6-methoxyquinolin-4-yl)oxy)phenyl)-4-oxo-1-(2-(trifluoromethyl)phenyl)-1,4-dihydropyridazine-3-carboxamide (**14a**)*

White solid; Yield: 79.1%; M.p.: 188-190 °C; HRMS (ESI) (m/z): $[M+H]^+$ calcd for $C_{30}H_{23}F_3N_5O_7$, 622.1466;

found, 622.1472; ^{1}H-NMR (400 MHz, DMSO-d_6) δ (ppm): 11.89 (s, 1H), 10.91 (s, 1H), 9.08 (s, 1H), 8.78 (d, J = 7.8 Hz, 1H), 8.48 (d, J = 5.3 Hz, 1H), 8.04 (d, J = 7.8 Hz, 1H), 7.98 (d, J = 7.6 Hz, 1H), 7.94–7.76 (m, 4H), 7.54 (s, 1H), 7.36 (s, 1H), 7.30 (d, J = 8.6 Hz, 2H), 6.94 (d, J = 7.7 Hz, 1H), 6.51 (d, J = 5.2 Hz, 1H), 4.65 (s, 2H), 3.95 (s, 3H). ^{13}C NMR (151 MHz, DMSO-*d6*) δ 169.18 , 163.86 , 159.75 , 159.18 , 151.10 , 150.00 , 149.30 ,148.94 , 147.44 , 146.08 ,144.93 , 140.57 , 135.52 ,134.38 , 131.21 , 129.05 , 127.69 , 123.74 , 121.92 ,121.64 , 121.57 , 119.57 , 115.59 ,109.07 , 103.41 , 99.38 , 66.05 , 55.72 .

4.1.12.2

*1-(3-chloro-4-(trifluoromethyl)phenyl)-N-(4-((7-(2-(hydroxyamino)-2-oxoethoxy)-6-methoxyquinolin-4-yl)oxy)phenyl)-5-methyl-4-oxo-1,4-dihydropyridazine-3-carboxamide (**14b**)*

Light yellow solid; Yield: 86.2%; M.p.: 182-184 ºC; HRMS (ESI) (m/z): $[M+H]^+$ calcd for $C_{31}H_{24}ClF_3N_5O_7$,

670.1245; found, 670.1250; ^{1}H-NMR (400 MHz, DMSO-d_6) δ (ppm): 11.99 (s, 1H), 10.90 (s, 1H), 9.21 (s, 1H), 9.07 (s, 1H), 8.49 (d, *J* = 5.3 Hz, 1H), 8.33 (d, *J* = 2.7 Hz, 1H), 8.19 (dd, *J* = 8.8, 2.7 Hz, 1H), 8.09–7.99 (m, 1H), 7.92–7.84 (m, 2H), 7.55 (s, 1H), 7.37 (s, 1H), 7.32 (d, *J* = 8.8 Hz, 2H), 6.53 (d, *J* = 5.3 Hz, 1H), 4.65 (s, 2H), 3.96 (s, 3H), 2.14 (s, 3H).

4.1.12.3

*N-(4-((7-(2-(hydroxyamino)-2-oxoethoxy)-6-methoxyquinolin-4-yl)oxy)phenyl)-5-methyl-4-oxo-1-(o-tolyl)-1,4-dihydropyridazine-3-carboxamide (**14c**)*

Light yellow solid; Yield: 87.5%; M.p.: 198-200 ºC; HRMS (ESI) (m/z): $[M+H]^+$ calcd for $C_{31}H_{28}N_5O_7$, 582.1962; found, 582.1972; ^{1}H NMR (400 MHz, DMSO-d_6) δ 12.52 (s, 1H), 11.96 (s, 1H), 10.91 (s, 1H), 9.09 (d, *J* = 1.6 Hz, 1H), 8.80 (d, *J* = 1.1 Hz, 1H), 8.49 (d, *J* = 5.3 Hz, 1H), 8.03 (dd, *J* = 12.8, 2.4 Hz, 1H), 7.61–7.41 (m, 7H), 7.37 (s, 1H), 6.52 (d, *J* = 5.2 Hz, 1H), 4.66 (s, 2H), 3.97 (s, 3H), 2.24 (s, 3H), 2.18 (s, 3H). ^{13}C NMR (151 MHz, DMSO-*d6*) δ 170.00 , 164.25 , 160.49 , 159.59 , 154.71 , 153.08 , 151.60 , 149.85 , 149.35 , 146.39 , 143.69 , 143.23 , 143.00 , 133.48 , 131.89 , 131.58 , 130.34 , 127.56 , 126.28 , 124.72 , 117.10 , 115.37 , 109.45 , 102.76 , 99.65 , 66.47 , 56.18 , 17.48 , 13.21 .

4.1.12.4

*N-(3-fluoro-4-((7-(4-(hydroxyamino)-4-oxobutoxy)-6-methoxyquinolin-4-yl)oxy)phenyl)-5-methyl-4-oxo-1-(o-tolyl)-1,4-dihydropyridazine-3-carboxamide (**14d**)*

Yellow solid; Yield: 70.0%; M.p.: 164-166 °C; HRMS (ESI) (m/z): $[M+H]^+$ calcd for $C_{33}H_{31}FN_5O_7$, 628.2105;

found, 628.2081; ^{1}H-NMR (400 MHz, DMSO-d_6) δ (ppm): 12.52 (s, 1H), 10.48 (s, 1H), 8.81 (s, 1H), 8.75 (s, 1H), 8.48 (d, *J* = 5.2 Hz, 1H), 8.03 (dd, *J* = 12.7, 2.4 Hz, 1H), 7.61–7.42 (m, 7H), 7.40 (s, 1H), 6.50 (d, *J* = 5.2 Hz, 1H), 4.16 (t, *J* = 6.4 Hz, 2H), 3.96 (s, 3H), 2.24 (s, 3H), 2.20 (t, *J* = 7.4 Hz, 2H), 2.12 (s, 3H), 2.05 (q, *J* = 6.9 Hz, 2H). ^{13}C NMR (151 MHz, DMSO-*d6*) δ 169.99 , 168.95 , 160.49 , 159.56 , 152.21 , 150.10 , 149.93 , 149.25 , 146.74 , 143.72 , 143.23 , 143.00 , 137.50 , 136.64 , 133.48 , 131.89 , 131.56 , 130.34 , 127.56 , 126.28 , 124.72 , 117.09 , 114.90 , 109.18 , 108.95 , 102.54 , 99.44 , 68.08 , 56.17 , 29.14 , 25.00 , 17.49 , 13.21 .

4.1.12.5

*N-(3-fluoro-4-((7-(4-(hydroxyamino)-4-oxobutoxy)-6-methoxyquinolin-4-yl)oxy)phenyl)-5-methyl-4-oxo-1-phenyl-1,4-dihydropyridazine-3-carboxamide (**14e**)*

Yellow solid; Yield: 80.1%; M.p.: 182-184 ºC; HRMS (ESI) (m/z): $[M+H]^+$ calcd for $C_{32}H_{29}FN_5O_7$, 614.1924;

found, 614.1901; ^{1}H-NMR (400 MHz, DMSO-d_6) δ (ppm): 12.30 (s, 1H), 10.46 (s, 1H), 9.11 (d, J = 1.1 Hz, 1H), 8.73 (d, J = 1.7 Hz, 1H), 8.48 (d, J = 5.2 Hz, 1H), 8.05 (dd, J = 12.8, 2.4 Hz, 1H), 7.88–7.81 (m, 2H), 7.64 (dd, J = 8.6, 7.2 Hz, 2H), 7.61–7.46 (m, 4H), 7.40 (s, 1H), 6.51 (d, J = 5.1 Hz, 1H), 4.16 (t, J = 6.4 Hz, 2H), 3.97 (s, 3H), 2.20 (t, J = 7.4 Hz, 2H), 2.15 (s, 3H), 2.04 (m, 2H). ^{13}C NMR (151 MHz, DMSO-*d6*) δ 170.06 , 168.96 , 160.64 , 159.58 , 154.74 , 153.11 , 152.21 , 149.94 , 149.25 , 146.73 , 144.47 , 143.41 , 140.02 , 137.51 , 131.84 , 130.11 , 129.04 , 124.75 , 121.83 , 117.04 , 114.89 , 109.11 , 108.95 , 102.52 , 99.44 , 68.08 , 56.19 , 29.14 , 24.99 , 13.34 .

4.1.12.6

*N-(3-fluoro-4-((7-(4-(hydroxyamino)-4-oxobutoxy)-6-methoxyquinolin-4-yl)oxy)phenyl)-4-oxo-1-(o-tolyl)-1,4-dihydropyridazine-3-carboxamide (**14f**)*

Yellow solid; Yield: 73.0%; M.p.:149-151 ºC; HRMS (ESI) (m/z): $[M+H]^+$ calcd for $C_{32}H_{29}FN_5O_7$, 614.2002;

found, 614.1985; ^{1}H-NMR (400 MHz, DMSO-d_6) δ 12.18 (s, 1H), 10.45 (s, 1H), 8.73 (s, 1H), 8.71 (d, J = 5.9 Hz, 1H), 8.48 (d, J = 5.2 Hz, 1H), 8.00 (dd, J = 12.7, 2.4 Hz, 1H), 7.58–7.42 (m, 7H), 7.40 (s, 1H), 6.93 (d, J = 7.7 Hz, 1H), 6.50 (d, J = 5.2 Hz, 1H), 4.16 (t, J = 6.5 Hz, 2H), 3.96 (s, 3H), 2.25 (s, 3H), 2.20 (t, J = 7.4 Hz, 2H), 2.04 (p, J = 7.0 Hz, 2H).

4.1.12.7

*N-(3-fluoro-4-((7-(4-(hydroxyamino)-4-oxobutoxy)-6-methoxyquinolin-4-yl)oxy)phenyl)-1-(2-fluorophenyl)-5-methyl-4-oxo-1,4-dihydropyridazine-3-carboxamide (**14g**)*

Yellow solid; Yield: 74.9%; M.p.: 164-166 °C; HRMS (ESI) (m/z): $[M+H]^+$ calcd for $C_{32}H_{28}F_2N_5O_7$, 632.1892;

found, 632.1874; ^{1}H-NMR (400 MHz, DMSO-d_6) δ 12.15 (s, 1H), 10.47 (s, 1H), 8.88 (s, 1H), 8.74 (s, 1H), 8.49 (d, J = 5.3 Hz, 1H), 8.01 (dd, J = 12.8, 2.5 Hz, 1H), 7.80 (t, J = 7.8 Hz, 1H), 7.71–7.43 (m, 6H), 7.40 (s, 1H), 6.51 (d, J = 5.4 Hz, 1H), 4.16 (t, J = 6.4 Hz, 2H), 3.97 (s, 3H), 2.20 (t, J = 7.4 Hz, 2H), 2.11 (s, 3H), 2.04 (m, 2H).

4.1.12.8

*1-(2-fluorophenyl)-N-(4-((7-(4-(hydroxyamino)-4-oxobutoxy)-6-methoxyquinolin-4-yl)oxy)phenyl)-5-methyl-4-oxo-1,4-dihydropyridazine-3-carboxamide (**14h**)*

White solid; Yield: 81.4%; M.p.:170-172 ºC; HRMS (ESI) (m/z): $[M+H]^+$ calcd for $C_{32}H_{29}FN_5O_7$, 614.1989;

found, 614.1976; ^{1}H-NMR (400 MHz, DMSO-d_6) δ (ppm): 12.06 (s, 1H), 10.48 (s, 1H), 8.87 (s, 1H), 8.76 (s, 1H), 8.48 (d, J = 5.2 Hz, 1H), 7.86 (d, J = 8.6 Hz, 2H), 7.80 (s, 1H), 7.71–7.42 (m, 3H), 7.39 (s, 1H), 7.31 (d, J = 8.5 Hz, 2H), 6.50 (d, J = 5.2 Hz, 1H), 4.16 (t, J = 6.4 Hz, 2H), 3.95 (s, 3H), 2.21 (t, J = 7.4 Hz, 2H), 2.11 (s, 3H), 2.05

(m, 2H). ^{13}C NMR (151 MHz, DMSO-*d6*) δ 169.92 , 168.99 , 160.23 , 160.03 , 155.93 , 154.27 , 152.16 , 150.32 , 149.81 , 149.14 , 146.67 , 145.48 , 142.78 , 136.09 , 132.06 , 131.58 , 130.92 , 127.68 , 125.90 , 122.03 , 121.87 , 117.53 , 117.40 , 115.54 , 108.84 , 103.60 , 99.59 , 68.06 , 56.12 , 29.15 , 25.01 , 13.16 .

4.1.12.9

*N-(4-((7-(4-(hydroxyamino)-4-oxobutoxy)-6-methoxyquinolin-4-yl)oxy)phenyl)-5-methyl-4-oxo-1-(o-tolyl)-1,4-dihydropyridazine-3-carboxamide (**14i**)*

Light yellow solid; Yield: 81.3%; M.p.: 187-189 ºC; HRMS (ESI) (m/z): $[M+H]^+$ calcd for $C_{33}H_{32}N_5O_7$, 610.2243; found, 610.2234; ^{1}H-NMR (400 MHz, DMSO-d_6) δ (ppm): δ 12.41 (s, 1H), 10.48 (s, 1H), 8.77 (d, *J* = 15.6 Hz, 2H), 8.48 (d, *J* = 5.2 Hz, 1H), 7.86 (d, *J* = 8.5 Hz, 2H), 7.61–7.42 (m, 5H), 7.38 (s, 1H), 7.31 (d, *J* = 8.5 Hz, 2H), 6.50 (d, *J* = 5.1 Hz, 1H), 4.16 (t, *J* = 6.4 Hz, 2H), 3.95 (s, 3H), 2.24 (s, 3H), 2.20 (t, *J* = 7.3 Hz, 2H), 2.12 (s, 3H), 2.05 (m, 2H). ^{13}C NMR (151 MHz, DMSO-*d6*) δ 170.10 , 168.99 , 160.16 , 160.08 , 152.13 , 150.31 , 149.79 , 149.20 , 146.77 , 143.77 , 143.26 , 142.89 , 136.10 , 133.49 , 131.86 , 131.46 , 130.30 , 127.53 , 126.28 , 122.02 , 121.90 , 115.55 , 108.93 , 103.61 , 99.58 , 68.05 , 56.11 , 29.16 , 25.02 , 17.49 , 13.22 .

4.1.12.10

*N-(4-((7-(4-(hydroxyamino)-4-oxobutoxy)-6-methoxyquinolin-4-yl)oxy)phenyl)-4-oxo-1-phenyl-1,4-dihydropyridazine-3-carboxamide (**14j**)*

Light yellow solid; Yield: 81.0%; M.p.: 172-174 ºC; HRMS (ESI) (m/z): $[M+H]^+$ calcd for $C_{31}H_{28}N_5O_7$, 582.1934; found, 582.1916; ^{1}H-NMR (400 MHz, DMSO-d_6) δ (ppm): 11.90 (s, 1H), 10.47 (s, 1H), 9.03 (d, *J* = 7.8 Hz, 1H), 8.75 (s, 1H), 8.48 (d, *J* = 5.2 Hz, 1H), 8.02–7.73 (m, 4H), 7.63 (t, *J* = 7.8 Hz, 2H), 7.56–7.47 (m, 2H), 7.38 (s, 1H), 7.32 (d, *J* = 8.8 Hz, 2H), 6.93 (d, *J* = 7.8 Hz, 1H), 6.50 (d, *J* = 5.2 Hz, 1H), 4.16 (t, *J* = 6.4 Hz, 2H), 3.95 (s, 3H), 2.20 (t, *J* = 7.4 Hz, 2H), 2.04 (t, *J* = 7.1 Hz, 2H). ^{13}C NMR (151 MHz, DMSO-*d6*) δ 169.21 , 168.56 , 159.78 , 159.71 , 151.72 , 149.94 , 149.39 , 148.83 , 147.98 , 146.38 , 142.88 , 141.74 , 135.69 , 129.71 , 128.58 , 121.67 , 121.45 , 121.36 , 120.36 , 115.12 , 108.54 , 103.19 , 99.18 , 67.64 , 55.72 , 28.73 , 24.60 .

4.1.12.11

*N-(3-fluoro-4-((7-((6-(hydroxyamino)-6-oxohexyl)oxy)-6-methoxyquinolin-4-yl)oxy)phenyl)-1-(2-fluorophenyl)-5-methyl-4-oxo-1,4-dihydropyridazine-3-carboxamide (**14k**)*

Yellow solid; Yield: 71.3%; M.p.: 167-169 °C; HRMS (ESI) (m/z): $[M+H]^+$ calcd for $C_{34}H_{32}F_2N_5O_7$, 660.2214;

found, 660.2202; ^{1}H NMR (600 MHz, DMSO-d_6) δ 12.17 (s, 1H), 10.38 (s, 1H), 8.88 (s, 1H), 8.71 (s, 1H), 8.48 (d, *J* = 5.3 Hz, 1H), 8.01 (dd, *J* = 12.7, 2.5 Hz, 1H), 7.80 (t, *J* = 7.8 Hz, 1H), 7.65 (d, *J* = 6.7 Hz, 1H), 7.62–7.53 (m,

3H), 7.49 (dt, *J* = 11.2, 8.2 Hz, 2H), 7.40 (s, 1H), 6.50 (d, *J* = 5.2 Hz, 1H), 4.15 (t, *J* = 6.4 Hz, 2H), 3.96 (s, 3H), 2.11 (s, 3H), 2.01 (t, *J* = 7.3 Hz, 2H), 1.82 (q, *J* = 7.2 Hz, 2H), 1.60 (p, *J* = 7.7 Hz, 2H), 1.45 (m, 2H). ^{13}C NMR (151 MHz, DMSO-*d6*) δ 169.37 , 168.99 , 160.03 , 159.16 , 153.86 , 151.95 , 149.55 , 148.78 , 146.36 , 145.07 , 142.46 , 137.01 , 136.26 , 131.70 , 131.21 , 130.62 , 127.27 , 125.53 , 124.34 , 117.15 , 117.03 , 116.64 , 114.40 , 108.72 , 108.44 , 102.08 , 98.96 , 68.21 , 55.76 , 32.21 , 28.22 , 25.19 , 24.88 , 12.75 .

4.1.12.12

*N-(3-fluoro-4-((7-((6-(hydroxyamino)-6-oxohexyl)oxy)-6-methoxyquinolin-4-yl)oxy)phenyl)-5-methyl-4-oxo-1-phenyl-1,4-dihydropyridazine-3-carboxamide (**14l**)*

White solid; Yield: 73.5%; M.p.: 134-136 ºC; HRMS (ESI) (m/z): $[M+H]^+$ calcd for $C_{34}H_{33}FN_5O_7$, 642.2298; found, 642.2279; ^{1}H NMR (600 MHz, DMSO-d_6) δ (ppm) 12.30 (s, 1H), 10.37 (s, 1H), 9.12 (s, 1H), 8.69 (s, 1H), 8.49 (d, *J* = 5.1 Hz, 1H), 8.05 (d, *J* = 12.8 Hz, 1H), 7.85 (d, *J* = 8.3 Hz, 2H), 7.67–7.48 (m, 6H), 7.41 (s, 1H), 6.51 (d, *J* = 5.3 Hz, 1H), 4.15 (t, *J* = 6.5 Hz, 2H), 3.97 (s, 3H), 2.15 (s, 3H), 2.01 (t, *J* = 7.3 Hz, 2H), 1.82 (t, *J* = 7.4 Hz, 2H), 1.60 (q, *J* = 7.4 Hz, 2H), 1.46 (q, *J* = 7.6 Hz, 2H) .

4.1.12.13

*N-(4-((7-((6-(hydroxyamino)-6-oxohexyl)oxy)-6-methoxyquinolin-4-yl)oxy)phenyl)-4-oxo-1-(o-tolyl)-1,4-dihydropyridazine-3-carboxamide (**14m**)*

Yellow green solid; Yield: 81.0%; M.p.: 137-139 ºC; HRMS (ESI) (m/z): $[M+H]^+$ calcd for $C_{34}H_{34}N_5O_7$, 624.2388; found, 624.2364; ^{1}H-NMR (400 MHz, DMSO-d_6) δ (ppm): 12.08 (s, 1H), 10.37 (s, 1H), 8.79 – 8.59 (m, 2H), 8.47 (d, *J* = 5.2 Hz, 1H), 7.84 (d, *J* = 8.6 Hz, 2H), 7.59–7.42 (m, 5H), 7.39 (s, 1H), 7.30 (d, *J* = 8.5 Hz, 2H), 6.92 (d, *J* = 7.6 Hz, 1H), 6.49 (d, *J* = 5.2 Hz, 1H), 4.14 (t, *J* = 6.6 Hz, 2H), 3.94 (s, 3H), 2.25 (s, 3H), 2.00 (t, *J* = 7.3 Hz, 2H), 1.81 (m, 2H), 1.67–1.55 (m, 2H), 1.45 (m, 2H). ^{13}C NMR (151 MHz, DMSO-*d6*) δ 169.22 , 169.01 , 159.79 ,159.52 , 151.90 , 149.96 , 149.42 , 148.71 , 147.21 , 146.34 , 144.65 , 142.69 , 135.59 , 133.10 , 131.48 , 129.92 , 127.18 , 125.90 , 121.65 , 121.52 , 120.03 , 115.05 ,108.36 , 103.15 , 99.12 , 68.18 , 55.70 , 32.21 , 28.23 , 25.20 , 24.89 , 17.11 .

4.1.12.14

*N-(4-((7-((6-(hydroxyamino)-6-oxohexyl)oxy)-6-methoxyquinolin-4-yl)oxy)phenyl)-5-methyl-4-oxo-1-(o-tolyl)-1,4-dihydropyridazine-3-carboxamide (**14n**)*

Yellow solid; Yield:78.5%; M.p.:175-177 ºC; HRMS (ESI) (m/z): $[M+H]^+$ calcd for $C_{35}H_{36}N_5O_7$, 638.2554; found, 638.2532; ^{1}H-NMR (400 MHz, DMSO-d_6) δ (ppm): 12.41 (s, 1H), 10.37 (s, 1H), 8.79 (s, 1H), 8.70 (s, 1H), 8.47 (d, *J* = 5.2 Hz, 1H), 7.86 (d, *J* = 8.9 Hz, 2H), 7.61–7.42 (m, 5H), 7.39 (s, 1H), 7.30 (d, *J* = 8.9 Hz, 2H), 6.50

(d, *J* = 5.2 Hz, 1H), 4.14 (t, *J* = 6.1 Hz, 2H), 3.94 (s, 3H), 2.24 (s, 3H), 2.12 (s, 3H), 2.01 (t, *J* = 7.2 Hz, 2H), 1.89–1.75 (m, 2H), 1.60 (p, *J* = 7.7, 7.3 Hz, 2H), 1.46 (q, *J* = 14.6, 13.7 Hz, 2H). ^{13}C NMR (151 MHz, DMSO-*d6*) *δ* 170.22 , 169.59 , 160.31 , 160.19 , 152.40 , 150.41 , 149.92 , 149.21 , 146.83 , 143.82 , 143.36 , 142.99 , 136.19 , 133.59 , 131.97 , 131.61 , 130.41 , 127.64 , 126.37 , 122.14 , 122.02 , 115.56 , 108.82 , 103.65 , 99.61 , 68.68 , 56.17 , 32.71 , 28.72 , 25.70 , 25.39 , 17.57 , 13.30 .

4.1.12.15

*N-(4-((7-((7-(hydroxyamino)-7-oxoheptyl)oxy)-6-methoxyquinolin-4-yl)oxy)phenyl)-5-methyl-4-oxo-1-phenyl-1,4-dihydropyridazine-3-carboxamide (**14o**)*

Yellow solid; Yield: 84.2%; M.p.: 143-144 ºC; HRMS (ESI) (m/z): $[M+H]^+$ calcd for $C_{35}H_{36}N_5O_7$, 638.2558; found, 638.2535; ^{1}H-NMR (400 MHz, DMSO-d_6) *δ* (ppm): 12.19 (s, 1H), 10.38 (s, 1H), 9.11 (s, 1H), 8.71 (s, 1H), 8.47 (d, *J* = 5.2 Hz, 1H), 7.86 (dd, *J* = 14.2, 8.4 Hz, 4H), 7.64 (t, *J* = 7.7 Hz, 2H), 7.52 (d, *J* = 3.5 Hz, 2H), 7.39 (s, 1H), 7.31 (d, *J* = 8.8 Hz, 2H), 6.50 (d, *J* = 5.2 Hz, 1H), 4.14 (t, *J* = 6.5 Hz, 2H), 3.94 (s, 3H), 2.14 (s, 3H), 1.99 (t, *J* = 7.2 Hz, 2H), 1.81 (t, *J* = 7.4 Hz, 2H), 1.60 (p, *J* = 7.4 Hz, 2H), 1.45 (q, *J* = 7.9 Hz, 2H). 1.35 (q, *J* = 7.3, 6.8 Hz, 2H). ^{13}C NMR (151 MHz, DMSO-*d6*) *δ* 170.17 , 169.48 , 160.25 , 160.17 , 152.29 , 150.32 , 149.83 , 149.17 , 146.82 , 144.60 , 143.44 , 139.93 , 136.17 , 131.69 , 130.09 , 128.99 , 122.05 , 121.84 ,121.83 , 115.45 , 108.82 , 103.57 , 99.52 , 68.61 , 56.11 , 32.62 , 28.76 , 28.72 , 25.68 , 25.46 , 13.35 .

4.1.12.16

*N-(4-((7-((7-(hydroxyamino)-7-oxoheptyl)oxy)-6-methoxyquinolin-4-yl)oxy)phenyl)-5-methyl-4-oxo-1-(o-tolyl)-1,4-dihydropyridazine-3-carboxamide (**14p**)*

Yellow solid; Yield: 83.7%; M.p.: 141-143 ºC; HRMS (ESI) (m/z): $[M+H]^+$ calcd for $C_{36}H_{38}N_5O_7$, 652.2724; found, 652.2715; ^{1}H NMR (600 MHz, DMSO-d_6) δ 12.41 (s, 1H), 10.37 (s, 1H), 8.79 (s, 1H), 8.47 (d, *J* = 5.1 Hz, 1H), 7.86 (d, *J* = 8.6 Hz, 2H), 7.55 (d, *J* = 7.6 Hz, 1H), 7.50 (dd, *J* = 10.8, 7.1 Hz, 3H), 7.45 (t, *J* = 6.9 Hz, 1H), 7.38 (s, 1H), 7.30 (d, *J* = 8.6 Hz, 2H), 6.49 (d, *J* = 5.1 Hz, 1H), 4.14 (t, *J* = 6.1 Hz, 2H), 3.94 (s, 3H), 2.24 (s, 3H), 2.12 (s, 3H), 1.98 (t, *J* = 7.2 Hz, 2H), 1.84 – 1.76 (m, 2H), 1.58–1.50 (m, 2H), 1.50–1.42 (m, 2H), 1.35 (q, *J* = 7.3, 6.8 Hz, 2H). ^{13}C NMR (151 MHz, DMSO-d_6) δ 170.09 , 169.45 , 160.14 , 160.10 , 152.28 , 150.33 ,149.83 , 149.17 , 146.84 , 143.84 , 143.27 , 142.91 , 136.09 , 133.50 , 131.87 , 131.43 , 130.31 , 127.54 , 126.29 , 122.03 , 121.90 , 115.46 , 108.84 , 103.58 , 99.51 , 68.60 , 56.10 , 32.62 , 28.76 , 28.73 , 25.68 , 25.47 , 17.49 , 13.22 .

4.1.12.17

*1-(3-chloro-4-fluorophenyl)-N-(4-((7-((7-(hydroxyamino)-7-oxoheptyl)oxy)-6-methoxyquinolin-4-yl)oxy)phenyl)-5-methyl-4-oxo-1,4-dihydropyridazine-3-carboxamide (**14q**)*

Yellow green solid; Yield: 80.2%; M.p.: 199-201 ºC; HRMS (ESI) (m/z): $[M+H]^+$ calcd for $C_{35}H_{34}ClFN_5O_7$, 690.2074; found, 690.2050; ^{1}H-NMR (400 MHz, DMSO-d_6) δ (ppm): 12.07 (s, 1H), 10.36 (s, 1H), 9.11 (s, 1H), 8.68 (s, 1H), 8.48 (d, *J* = 5.2 Hz, 1H), 8.16 (dd, *J* = 6.4, 2.8 Hz, 1H), 7.93–7.82 (m, 3H), 7.72 (t, *J* = 9.0 Hz, 1H), 7.53 (s, 1H), 7.39 (s, 1H), 7.35–7.27 (m, 2H), 6.51 (d, *J* = 5.2 Hz, 1H), 4.14 (t, *J* = 6.6 Hz, 2H), 3.95 (s, 3H), 2.12 (s, 3H), 1.97 (t, *J* = 7.3 Hz, 2H), 1.81 (t, *J* = 7.3 Hz, 2H), 1.53 (t, *J* = 7.4 Hz, 2H), 1.46 (m, 2H), 1.36 (t, *J* = 7.6 Hz, 2H).

4.1.12.18

*1-(2,4-dimethylphenyl)-N-(4-((7-((7-(hydroxyamino)-7-oxoheptyl)oxy)-6-methoxyquinolin-4-yl)oxy)phenyl)-5-methyl-4-oxo-1,4-dihydropyridazine-3-carboxamide (**14r**)*

Yellow green solid; Yield: 41.2%; M.p.: 152-154 ºC; HRMS (ESI) (m/z): $[M+H]^+$ calcd for $C_{37}H_{40}N_5O_7$, 666.2863; found, 666.2858; ^{1}H NMR (600 MHz, DMSO-d_6) δ 12.43 (s, 1H), 10.35 (s, 1H), 8.76–8.72 (m, 1H), 8.68 (s, 1H), 8.47 (d, *J* = 5.2 Hz, 1H), 7.86 (d, *J* = 8.9 Hz, 2H), 7.51 (s, 1H), 7.42 (d, *J* = 8.0 Hz, 1H), 7.38 (s, 1H), 7.33–7.27 (m, 3H), 7.26–7.21 (m, 1H), 6.49 (d, *J* = 5.2 Hz, 1H), 4.14 (t, *J* = 6.5 Hz, 2H), 3.94 (s, 3H), 2.38 (s, 3H), 2.19 (s, 3H), 2.11 (s, 3H), 1.97 (t, *J* = 7.4 Hz, 2H), 1.81 (p, *J* = 6.7 Hz, 2H), 1.54 (p, *J* = 7.5 Hz, 2H), 1.46 (p, *J* = 7.6 Hz, 2H), 1.35 (q, *J* = 8.2 Hz, 2H). ^{13}C NMR (151 MHz, DMSO-*d6*) *δ*170.06 , 169.49 , 160.15 , 160.09 , 152.29 , 150.31 , 149.83 , 149.15 , 146.82 , 143.71 , 142.98 , 141.04 , 139.95 , 136.10 , 133.11 , 132.20 , 131.47 , 127.88 , 126.03 , 122.02 , 121.88 , 115.46 , 108.81 , 103.56 , 99.51 , 68.60 , 56.09 , 32.62 , 28.76 , 28.73 , 25.68 , 25.47 , 21.00 , 17.40 , 13.21 .

4.1.12.19

*N-(4-((7-((7-(hydroxyamino)-7-oxoheptyl)oxy)-6-methoxyquinolin-4-yl)oxy)phenyl)-5-methyl-4-oxo-1-(3-(trifluoromethyl)phenyl)-1,4-dihydropyridazine-3-carboxamide (**14s**)*

White solid; Yield: 80.6%; M.p.:152-154 ºC; HRMS (ESI) (m/z): $[M+H]^+$ calcd for $C_{36}H_{35}F_3N_5O_7$, 706.2441; found, 706.2422; ^{1}H-NMR (400 MHz, DMSO-d_6) δ (ppm): 12.08 (s, 1H), 11.95 (s, 1H), 10.36 (s, 1H), 9.21 (s, 1H), 8.47 (d, *J* = 5.2 Hz, 1H), 8.21 (d, *J* = 22.8 Hz, 2H), 7.88 (d, *J* = 8.1 Hz, 2H), 7.67–7.62 (m, 2H), 7.52 (m, 2H), 7.30–7.38 (m, 4H), 6.50 (d, *J* = 5.2 Hz, 1H), 4.14 (t, *J* = 6.4 Hz, 2H), 3.95 (s, 3H), 2.14 (s, 3H), 1.98 (t, *J* = 7.2 Hz, 2H), 1.81 (t, *J* = 7.3 Hz, 2H), 1.47 (t, *J* = 7.2 Hz, 2H), 1.35 (q, *J* = 7.5, 6.8 Hz, 2H). ^{13}C NMR (151 MHz, DMSO-*d6*) *δ* 169.88 , 169.08 , 159.75 , 159.70 , 151.88 , 149.97 , 149.43 , 148.77 , 146.43 , 144.59 , 143.34 , 139.40 , 135.69 , 131.10 , 131.00 , 130.17 ,125.33 , 125.03 ,121.64 , 121.46 , 118.06 , 118.03 ,115.05 , 108.42 , 103.17 , 99.11 , 68.20 , 55.70 , 32.21 , 28.35 , 28.32 , 25.27 , 25.06 , 12.88 .

4.1.12.20

*N-(3-fluoro-4-((7-((7-(hydroxyamino)-7-oxoheptyl)oxy)-6-methoxyquinolin-4-yl)oxy)phenyl)-5-methyl-4-oxo-1-(o-tolyl)-1,4-dihydropyridazine-3-carboxamide (**14t**)*

White solid; Yield: 82.3%; M.p.: 159-161 ºC; HRMS (ESI) (m/z): $[M+H]^+$ calcd for $C_{36}H_{37}FN_5O_7$, 670.2622; found, 670.2605; ^{1}H NMR (600 MHz, DMSO-d_6) δ 12.52 (s, 1H), 10.36 (s, 1H), 8.80 (s, 1H), 8.69 (s, 1H), 8.48 (d, *J* = 5.2 Hz, 1H), 8.03 (dd, *J* = 12.7, 2.4 Hz, 1H), 7.63–7.42 (m, 7H), 7.40 (s, 1H), 6.49 (d, *J* = 5.2 Hz, 1H), 4.15 (t, *J* = 6.5 Hz, 2H), 3.96 (s, 3H), 2.24 (s, 3H), 2.12 (s, 3H), 1.98 (t, *J* = 7.3 Hz, 2H), 1.81 (t, *J* = 7.4 Hz, 2H), 1.54 (t, *J* = 7.5 Hz, 2H), 1.51–1.42 (m, 2H), 1.38–1.30 (m, 2H). ^{13}C NMR (151 MHz, DMSO-*d6*) *δ* 170.01 , 169.48 , 160.47 , 159.56 , 153.10 , 152.36 , 149.97 , 149.19 , 146.78 , 143.67 , 143.23 , 142.99 , 137.48 ,136.43 , 133.48 , 131.89 , 131.59 , 130.34 , 127.56 , 126.28 , 124.72 , 117.09 , 114.81 , 109.18 ,108.83 , 102.48 , 99.36 , 68.64 , 56.16 , 32.61 , 28.75 , 28.72 , 25.67 , 25.46 , 17.48 , 13.21 .

4.1.12.21

*N-(3-fluoro-4-((7-((7-(hydroxyamino)-7-oxoheptyl)oxy)-6-methoxyquinolin-4-yl)oxy)phenyl)-4-oxo-1-(o-tolyl)-1,4-dihydropyridazine-3-carboxamide (**14u**)*

White solid; Yield: 78.2%; Mp: 138-140 °C; HRMS (ESI) (m/z): $[M+H]^+$ calcd for $C_{35}H_{35}FN_5O_7$, 656.2420; found, 656.2402; ^{1}H-NMR (400 MHz, DMSO-d_6) δ (ppm) 12.19 (s, 1H), 11.93 (s, 1H), 10.35 (s, 1H), 8.72 (d, *J* = 7.5 Hz, 1H), 8.68 (s, 1H), 8.48 (d, *J* = 5.2 Hz, 1H), 8.00 (dd, *J* = 12.8, 2.2 Hz, 1H), 7.58–7.46 (m, 6H), 7.40 (s, 1H), 6.93 (d, *J* = 7.5 Hz, 1H), 6.49 (d, J = 5.0 Hz, 1H), 4.15 (t, *J* = 6.5 Hz, 2H), 3.96 (s, 3H), 2.25 (s, 3H), 1.97 (t, *J* = 7.3 Hz, 2H), 1.81 (m, 2H), 1.54 (t, *J* = 7.4 Hz, 2H), 1.50-1.43 (m, 2H), 1.35 (q, *J* = 7.6 Hz, 2H). ^{13}C NMR (151 MHz, DMSO-*d6*) *δ* 169.50 , 160.29 , 159.56 , 154.73 , 153.09 , 152.36 , 149.97 , 149.17 , 147.47 , 146.78 , 145.15 , 143.05 , 137.31 , 136.70 , 133.48 , 131.90 , 130.35 , 127.60 , 126.29 , 124.74 , 120.55 , 117.11 , 114.81 , 109.03 , 108.83 , 102.46 , 99.36 , 68.64 , 56.16 , 32.62 , 28.75 , 28.72 , 25.67 , 25.47 , 17.51 .

4.1.12.22

*N-(4-((7-((7-(hydroxyamino)-7-oxoheptyl)oxy)-6-methoxyquinolin-4-yl)oxy)phenyl)-5-methyl-4-oxo-1-(m-tolyl)-1,4-dihydropyridazine-3-carboxamide (**14v**)*

Yellow solid; Yield: 70.0%; Mp: 128-130 °C; HRMS (ESI) (m/z): $[M+H]^+$ calcd for $C_{36}H_{38}N_5O_7$, 652.2720; found, 652.2704; ^{1}H-NMR (400 MHz, DMSO-d_6) δ (ppm) 12.21 (s, 1H), 10.36 (s, 1H), 9.09 (s, 1H), 8.69 (s, 1H), 8.48 (d, *J* = 5.2 Hz, 1H), 7.88 (d, *J* = 8.9 Hz, 2H), 7.71–7.57 (m, 2H), 7.56–7.44 (m, 2H), 7.44–7.23 (m, 4H), 6.50 (d, *J* = 5.2 Hz, 1H), 4.14 (t, *J* = 6.5 Hz, 2H), 3.94 (s, 3H), 2.44 (s, 3H), 2.14 (s, 3H), 1.98 (t, *J* = 7.3 Hz, 2H), 1.87–1.74 (m, 2H), 1.53 (q, *J* = 7.6 Hz, 2H), 1.46 (q, *J* = 7.9 Hz, 2H), 1.35 (q, *J* = 8.2 Hz, 2H). ^{13}C NMR (151 MHz, DMSO-*d6*) *δ* 170.17 , 169.49 , 160.24 , 160.22 , 152.31 , 150.30 , 149.84 , 149.11 , 146.74 , 144.44 , 143.40 ,

139.86 , 139.83 , 136.18 , 131.72 , 129.88 , 129.58 , 122.15 , 122.04 , 121.83 , 118.89 , 115.45 , 108.74 , 103.57 , 99.52 , 68.61 , 56.11 , 32.62 , 28.76 , 28.73 , 25.68 , 25.47 , 21.34 , 13.32 .

4.1.12.23

*N-(4-((7-((7-(hydroxyamino)-7-oxoheptyl)oxy)-6-methoxyquinolin-4-yl)oxy)phenyl)-5-methyl-4-oxo-1-(p-tolyl)-1,4-dihydropyridazine-3-carboxamide (**14w**)*

Light yellow solid; Yield: 78.3%; M.p.: 203-204ºC; HRMS (ESI) (m/z): $[M+H]^+$ calcd for $C_{36}H_{38}N_5O_7$, 652.2726; found, 652.2706; ^{1}H-NMR (400 MHz, DMSO-d_6) δ (ppm): 12.23 (s, 1H), 10.37 (s, 1H), 9.08 (s, 1H), 8.47 (d, *J* = 5.2 Hz, 1H), 8.06 (s, 1H), 7.88 (d, *J* = 8.9 Hz, 2H), 7.76–7.70 (m, 2H), 7.52 (s, 1H), 7.43 (d, *J* = 8.3 Hz, 2H), 7.38 (s, 1H), 7.36–7.27 (m, 2H), 6.50 (d, *J* = 5.2 Hz, 1H), 4.14 (t, *J* = 6.6 Hz, 2H), 3.94 (s, 3H), 2.40 (s, 3H), 2.14 (s, 3H), 1.98 (q, *J* = 7.2 Hz, 2H), 1.82 (d, *J* = 8.5 Hz, 2H), 1.54 (t, *J* = 7.3 Hz, 2H), 1.46 (s, 2H), 1.38–1.31 (m, 2H). ^{13}C NMR (101 MHz, DMSO-d_6) δ 169.70 , 169.04 , 159.87 , 159.76 , 151.88 , 149.43 , 149.90 , 148.78 , 146.44 , 144.00 , 140.83 , 139.43 , 138.27 , 135.78 , 131.35 , 130.03 , 121.65 , 121.42 , 121.17 , 115.04 , 108.43 , 103.17 , 99.11 , 68.20 , 55.70 , 32.21 , 28.35 , 28.32 , 25.27 , 25.06 , 20.50 , 12.93 .

4.1.12.24

*N-(4-((7-((7-(hydroxyamino)-7-oxoheptyl)oxy)-6-methoxyquinolin-4-yl)oxy)phenyl)-4-oxo-1-phenyl-1,4-dihydropyridazine-3-carboxamide (**14x**)*

Light yellow solid; Yield: 58.3%; M.p.: 215-217 ºC; HPLC purity: 99.52%, retention time = 21.267 min. HRMS (ESI) (m/z): $[M+H]^+$ calcd for $C_{34}H_{34}N_5O_7$, 624.2359; found, 652.2330; ^{1}H-NMR (400 MHz, DMSO-d_6) δ (ppm): 11.90 (s, 1H), 10.36 (s, 1H), 9.03 (d, *J* = 7.8 Hz, 1H), 8.68 (s, 1H), 8.47 (d, *J* = 5.2 Hz, 1H), 7.93–7.76 (m, 4H), 7.63 (t, *J* = 7.7 Hz, 2H), 7.57–7.48 (m, 2H), 7.38 (s, 1H), 7.36–7.26 (m, 2H), 6.93 (d, *J* = 7.8 Hz, 1H), 6.49 (d, *J* = 5.2 Hz, 1H), 4.14 (t, *J* = 6.5 Hz, 2H), 3.94 (s, 3H), 1.97 (t, *J* = 7.3 Hz, 2H), 1.81 (t, *J* = 7.4 Hz, 2H), 1.51 (dq, *J* = 31.1, 8.2, 7.7 Hz, 4H), 1.35 (q, *J* = 7.5 Hz, 2H). ^{13}C NMR (151 MHz, DMSO-*d6*) δ 169.61 , 169.48，160.17 , 160.11 , 152.28 , 150.36 , 149.84 , 149.17 , 148.38 , 146.84 , 143.28 , 142.14 , 136.09 , 130.11 , 128.98 , 122.07 , 121.85 , 121.77 , 120.76 , 115.44 ,108.84 , 103.54 , 99.52 , 68.60 , 56.11 , 32.62 , 28.76 , 28.73 , 25.68 , 25.47 .

4.1.12.25

*5-ethyl-N-(4-((7-((7-(hydroxyamino)-7-oxoheptyl)oxy)-6-methoxyquinolin-4-yl)oxy)phenyl)-4-oxo-1-phenyl-1,4-dihydropyridazine-3-carboxamide (**14y**)*

Light yellow solid; Yield: 78.3%; M.p.: 185-187 ºC; HRMS (ESI) (m/z): $[M+H]^+$ calcd for $C_{36}H_{38}N_5O_7$, 652.2722; found, 652.2710; ^{1}H-NMR (400 MHz, DMSO-d_6) δ (ppm): 12.15 (s, 1H), 10.36 (s, 1H), 8.96 (s, 1H),

8.68 (s, 1H), 8.48 (d, *J* = 5.2 Hz, 1H), 7.87 (dd, *J* = 16.2, 8.1 Hz, 4H), 7.64 (t, *J* = 7.7 Hz, 2H), 7.53 (d, *J* = 6.3 Hz, 2H), 7.38 (s, 1H), 7.31 (d, *J* = 8.5 Hz, 2H), 6.50 (d, *J* = 5.1 Hz, 1H), 4.13 (q, *J* = 9.2, 7.8 Hz, 2H), 3.94 (s, 3H), 2.59 (q, *J* = 7.5 Hz, 2H), 1.98 (t, *J* = 7.3 Hz, 2H), 1.81 (t, *J* = 7.5 Hz, 2H), 1.54 (p, *J* = 7.4 Hz, 2H), 1.46 (p, *J* = 7.6 Hz, 2H), 1.34 (p, *J* = 7.6, 7.2 Hz, 2H), 1.21 (t, *J* = 7.5 Hz, 3H). ^{13}C NMR (151 MHz, DMSO-d_6) δ 169.60 , 169.48 , 160.33 , 160.18 , 152.29 , 150.32 , 149.84 , 149.19 , 146.83 , 145.32 , 143.55 , 139.20 , 136.65 , 136.17 , 130.07 , 128.99 , 122.05 , 121.99 , 121.85 , 115.46 , 108.83 , 103.58 , 99.53 , 68.61 , 56.11 , 32.62 , 28.76 , 28.72 , 25.68 , 25.46 , 20.61 , 12.56 .

4.2. Pharmacology

4.2.1. In vitro antiproliferative assays

The antiproliferative activities of compounds **14a-14y** were evaluated against HCT-116, MCF-7 and A549 cell lines by the standard MTT assay in vitro, with SAHA，AC-386 and Cabozantinib as the positive controls. The cancer cell lines were cultured in minimum essential medium (MEM) supplement with 10% fetal bovine serum (FBS). Approximate 4×10^3 cells, suspended in MEM medium, were plated into each well of a 96-well plate and incubated in 5% CO_2 at 37 °C for 24 h. The tested compounds at the indicated final concentrations were added to the culture medium and incubated for 72 h. Fresh MTT was added to each well at the terminal concentration of 5 μg/mL, and incubated with cells at 37 °C for 4 h. The formazan crystals in each well were dissolved in 100 μL DMSO, and the absorbency at 492 nm (for absorbance of MTT formazan) and 630 nm (for the reference wavelength) was measured with an ELISA reader. All of the compounds were tested three times in each of the cell lines. The results, expressed as IC_{50} (inhibitory concentration 50%), were the averages of three determinations and calculated relative to the vehicle (DMSO) control by the Bacus Laboratories Incorporated Slide Scanner (Bliss) software.

4.2.2 In vitro enzymatic assays

4.2.2.1 In vitro HDAC1 enzymatic assays

The following materials were purchased : HDAC1 (BPS, Cat. No. 50051), 384-well plate (Perkin Elmer, Cat. No. 6007279). The compounds were dissolved into 10 mM stock in 100% DMSO.

4.2.2.1.1 Experimental Methods

Prepare 1x assay buffer (modified Tris Buffer), then transfer compounds to assay plate by Echo in 100% DMSO. The final fraction of DMSO is 1%. Then we need to prepare enzyme solution in 1x assay buffer. Adding trypsin and Ac-peptide substrate in 1x assay buffer to make the substrate solution. Transfer 15 μL of enzyme

solution to assay plate or for low control transfer 15 µL of 1x assay buffer. Reactions were incubated for 15 min at room temperature and added 10 µL of substrate solution to each well to start reaction. Read the plate on Synergy MX with excitation at 355 nm and emission at 460 nm after incubating for another 60 min at room temperature.

4.2.2.1.2 Curve fitting

Fit the data in Excel to obtain inhibition values using equation (1)

Equation (1): Inh %=(Max-Signal)/ (Max-Min)*100

Fit the data in XL-Fit to obtain IC_{50} values using equation (2)

Equation (2): Y=Bottom + (Top-Bottom)/(1+(IC_{50}/X)*HillSlope)

Y is %inhibition and X is compound concentration.

4.2.2.2 In vitro c-Met enzymatic assays

The target compounds were tested for their activity against c-Met Tyrosine kinases through the mobility shift assay [32-33]. All kinase assays were performed in 96-well plates in a 50 µL reaction volume. The kinase buffer contains 50 mM HEPES, pH 7.5, 10 mM $MgCl_2$, 0.0015% Brij-35 and 2 mM DTT. The stop buffer contains 100 mM HEPES, pH 7.5, 0.015% Brij-35, 0.2% Coating Reagent 3 and 50 mM EDTA. Dilute the compounds to 500 µM by 100% DMSO, then transfer 10 µL of compound to a new 96-well plate as the intermediate plate, add 90 µL kinase buffer to each well. Transfer 5 µL of each well of the intermediate plate to 384-well plates. The following amounts of enzyme and substrate were used per well: kinase base buffer, FAM-labeled peptide, ATP and enzyme solution. Wells containing the substrate, enzyme, DMSO without compound were used as DMSO control. Wells containing just the substrate without enzyme were used as low control. Incubate at room temperature for 10 min. Add 10 µL peptide solution to each well. Incubate at 28 °C for specified period of time and stop reaction by 25 µL stop buffer. At last collect data on Caliper program and convert conversion values to inhibition values. Percent inhibition = (max − conversion)/(max − min)× 100. ‘max’ stands for DMSO control; ‘min’ stands for low control

4.2.3 Flow cytometry

The HCT-116 cells were seeded in 6-well plates at a seeding density of 105 cells per mL. Twelve hours later, various concentrations of compound **14x** were added. Cells were treated with compound **14x** for 48 h. Then cells were transferred to EP tubes and washed three times with PBS buffer. Then the procedures according to the operating instructions of the kit were followed. Ultimately, cell apoptosis was analyzed using Annexin-V and propidium iodide (PI) double staining by flow cytometry. Early apoptotic cells were defined as Annexin-V positive/PI negative, late apoptotic cells as Annexin-V/PI-double positive and necrotic cells as Annexin-V positive/PI positive.

4.2.4 Cell cycle distribution analysis

The effects of compounds on cell cycle progression were determined using a standard propidium iodide (PI) staining procedure followed by flow cytometry analysis. Briefly, HCT-116 cells were seeded in six-well plates (5×10^4/well) and then treated with different concentrations of **14x** for 48 h. The cells were collected and washed twice with ice cold PBS, then fixed in ice-cold 70% (v/v) ethanol overnight at 4 □. The cells were washed again by PBS, and then the cell DNA was stained with 400 μL PI (Beyotime) for 10 min. Data acquisition and analysis were performed using a flow cytometer.

4.2.5 Molecular docking study

The crystal structure of c-Met (PDB entry code: 3LQ8) in complex with XL880 and HDACs (PDB entry code: 1C3S) in complex with SAHA were used for molecular modeling. The protein structures were prepared using the protein preparation wizard in Maestro with standard settings. Grids were generated using glide, version 4.5.208, following the standard procedure recommended by Schrödinger software package version 2014. The conformational ensembles were docked flexibly using Glide with standard settings in both standard and extra precision mode. Only poses with low energy conformations and good hydrogen bond geometries were considered. The pictures elucidating the protein-ligand interactions were produced by Pymol (version 1.7.2.1).

Notes

The authors declare no competing financial interest.

Acknowledgements

This work was supported by grant (No. 81573295) from the National Natural Science Foundation of China and LiaoNing Revitalization Talents Program (XLYC1808037).

References

[1] G. Christensen, J. Burrows, R. Salgia, c-Met as a target for human cancer and characterization of inhibitors for therapeutic intervention, *Cancer Lett.* **2005**, 225, 0-26.

[2] J.R. Sierra, M-S. Tsao, c-Met as a potential therapeutic target and biomarker in cancer, *Ther. Adv. Med. Oncol*. **2011**, 3, 21-35.

[3] P.C. Ma, M.S. Tretiakova, V. Nallasura, R. Jagadeeswaran, A.N. Husain, R. Salgia, Downstream signalling and specific inhibition of c-Met/HGF pathway in small cell lung cancer: implications for tumour invasion, *Br. J. Cancer*. **2007**,97, 368-377.

[4] https://integrity.clarivate.com/integrity/xmlxsl/pk_prod_list.xml_prod_list_card_pr?p_id=379934&p_tsearch=

[5] P. K. Parikh, M. D. Ghate, Recent advances in the discovery of small molecule c-Met Kinase inhibitors, *Eur. J. Med. Chem.* **2018**, 143, 1103-1138.

[6] Lu. S, Preliminary efficacy and safety results of savolitinib treating patients with pulmonary sarcomatoid carcinoma (PSC) and other types of non-small cell lung cancer (NSCLC) harboring MET exon 14 skipping mutations, *AACR*. Atlanta, **2019**.

[7] L. V. Sequist, TATTON Phase Ib expansion cohort: Osimertinib plus savolitinib for patients (pts) with EGFR-mutant, MET-amplified NSCLC after progression on prior third-generation epidermal growth factor receptor (EGFR) tyrosine kinase inhibitor (TKI), *AACR*. Atlanta, **2019**.

[8] H. Yu, TATTON Phase Ib expansion cohort: Osimertinib plus savolitinib for patients (pts) with EGFR-mutant, MET amplified NSCLC after progression on prior first/secondgeneration epidermal growth factor receptor (EGFR) tyrosine kinase inhibitor (TKI), *AACR*. Atlanta, **2019**

[9] G.W. Collie, C. M. Koh, D. J. O'Neill, C. J. Stubbs, P. Khurana, A. Eddershaw, A. Snijder, F. Mauritzson, L. Barlind, I. L. Dale, J. Shaw, C. Phillips, E. J. Hennessy, T. Cheung, A. J Narvaez, Structural and Molecular Insight into Resistance Mechanisms of First Generation cMET Inhibitors, *ACS. Med. Chem. Lett.* **2019**, 10, 1322-1327.

[10] T. Reungwetwattana, Y. Liang, V. Zhu, S. I. Ou, The race to target MET exon 14 skipping alterations in non-small cell lung cancer: The Why, the How, the Who, the Unknown, and the Inevitable. *Lung cancer.* **2017**, *103*, 27-37.

[11] M. Bahcall, T. Sim, C. P. Paweletz, J. D. Patel, R. S. Alden, Y. Kuang, A. G. Sacher, N. D. Kim, C. A. Lydon, M. M. Awad, M. T. Jaklitsch, L. M. Sholl, P. A. Janne, G. R. Oxnard, Acquired METD1228V Mutation and Resistance to MET Inhibition in Lung Cancer. *Cancer discov.* **2016**, *6*, 1334-1341

[12] F. F. Wagner, U. M. Weiwer, M. C. Lewis, E. B. Holson, Small molecule inhibitors of zinc-dependent histone deacetylases, *Neurotherapeutics.* **2013**, 10, 589-604.

[13] O. Witt, H. E. Deubzer, T. Milde, I. Oehme, HDAC family: What are the cancer relevant targets? *Cancer Lett.* **2009**, 277, 8-21.

[14] S. J. Conway, P. M. Woster, J. K. Shen, G. Georg, S. Wang, Epigenetics: novel therapeutics targeting epigenetics, *J. Med. Chem.* **2015**, 58, 523-524.

[15] M. Guha, HDAC inhibitors still need a home run, despite recent approval, *Nat. Rev. Drug Discovery.* **2015**, 14, 225-226.

[16] E. Choy, Y. Flamand, S. Balasubramanian, J. E. Butrynski, D. C. Harmon, S. George, G. M. Cote, A. J. Wagner, J. A. Morgan, M. Sirisawad, C. Mani, F. J. Hornicek, Z. Duan, G. D. Demetri, Phase 1 study of oral abexinostat, a histone deacetylase inhibitor, in combination with doxorubicin in patients with metastatic sarcoma, *Cancer.* **2015**, 121, 1223-1230.

[17] J. R. Whittle, J. Desai, Histone deacetylase inhibitors in cancer: what have we learned? *Cancer.* **2015**, 121, 1164-1167.

[18] Y. Matsumoto, T. Motoki, S. Kubota, M. Takigawa, H. Tsubouchi, E. Gohda, Inhibition of tumor-stromal interaction through HGF/Met signaling by valproic acid, *Biochem. Biophys. Res.Commun.* **2008**, 366, 110-6.

[19] P. Bali, M. Pranpat, J. Bradner, M. Balasis, W. Fiskus, F. Guo, K. Rocha, S. Kumaraswamy, S. Boyapalle, P. Atadja, E. Seto, K. Bhalla, Inhibition of histone deacetylase 6 acetylates and disrupts the chaperone function of heat shock protein 90: a novel basis for antileukemia activity of histone deacetylase inhibitors, *J. Biol. Chem.*
2005, 280, 26729-26734.

[20] J. H. Kalin, J. A. Bergman, Development and therapeutic implications of selective histone deacetylase 6 inhibitors, *J. Med. Chem.* **2013**, 56, 6297-6313.

[21] D. Lu, J. Yan, L. Wang, H. C. Liu, L.M. Zeng, M. M. Zhang, W. W. Duan, Y. C. Ji, J.C. Cao, M.Y. Geng, A. J. Shen, Y. H. Hu, Design, Synthesis, and Biological Evaluation of the First c□Met/HDAC Inhibitors Based on Pyridazinone Derivatives, *ACS. Med. Chem. Lett.* **2017**, 8, 830-834.

[22] X. L. Shi, L. J. Wang, L. X. Ren, Y. Yuan. Preparation of dihydropyridazinone-containing quinoline compounds as anti-proliferative agents. CN105461687A. (2016).

[23] M. Finnin, J. Donigian, A. Cohen, V. Richon, R. Rifkind, P. Marks, R. Breslow, N. Pavletich, Structures of a histone deacetylase homologue bound to the TSA and SAHA inhibitors, *Nature*. **1999**, 401,188-193.

[24] T. A. Miller, D. J. Witter, S. Belvedere, Histone deacetylase inhibitors, *J. Med. Chem.* **2003**, 46, 5097-5116.

[25] A. B. Farag, H. A. Ewida, M. S. Ahmed. Design, synthesis, and biological evaluation of novel amide and hydrazide based thioether analogs targeting Histone deacteylase (HDAC) enzymes[J]. *Eur. J. Med. Chem*, **2018** 148, 73-85.

[26] X.Y. Li, Y. Q. Jiang, Y. K. Peterson, T. Q. Xu, R. A. Himes, X. Luo, G. L. Yin, E. S. Inks, N. Dolloff, S. Halene, S. S. L. Chan, C. J. Chou. Design of Hydrazide-Bearing HDACIs Based on Panobinostat and Their p53 and FLT3-ITD Dependency in Antileukemia Activity[J]. *J. Med. Chem.* **2020,** 63, 5501–5525.

[27] J. Zang, X. Liang, Y. Huang, Y, Jia, X. Li, W. Xu, C. J. Chou, Y. Zhang, Discovery of Novel Pazopanib-based HDAC and VEGFR Dual Inhibitors Targeting Cancer Epigenetics and Angiogenesis Simultaneously, *J. Med. Chem*. **2018**, 61, 5304-5322.

[28] S. Zhou, H. Liao, C. He, Y. Dou, M. Jiang, L. Ren, Y. Zhao, P. Gong, Design, synthesis and structure–relationships of novel 4-phenoxyquinoline derivatives containing pyridazinone moiety as potential antitumor agents, *Eur. J. Med. Chem*. **2014**, 83, 581-593.

[29] B. Qi, H. Tao, D. Wu, J. Bai, Y. Shi, P. Gong, Synthesis and Biological Evaluation of 4-Phenoxy-6,7-disubstituted Quinolines Possessing Semicarbazone Scaffolds as Selective c-Met Inhibitors, *Arch. Pharm. Chem. Life Sci.* **2013**, 346, 596-609.

[30] F. W. Peng, J. Xuan, T. T. Wu, J. Y. X, Z. W. Ren, D. K. Liu, X. Q. Wang, X. H. Chen, J. W. Zhang, Y. G. Xu, L. Shi, Design, synthesis and biological evaluation of N-phenylquinazolin-4-amine hybrids as dual inhibitors of VEGFR-2 and HDAC, *Eur. J. Med. Chem*. **2016**, 109, 1-12.

[31] F. Qian, S. Engst, K. Yamaguchi, P. Yu, K. Won, L. Mock, T. Lou, J. Tan, C. Li, D. Tam, Inhibition of Tumor Cell Growth, Invasion, and Metastasis by EXEL-2880 (XL880, GSK1363089), a Novel Inhibitor of HGF and VEGF Receptor Tyrosine Kinases, *Cancer Res.* **2009**, 69, 8009-8016.

[32] B. K. Albrecht, J. C. Harmange, D. Bauer, L. Berry, C. Bode, A. A. Boezio, A. Chen, D. Choquette, Dussault, I. C. Fridrich, R. Shimanovich, S. K. Springer, Y. Teffera, Y. Yang, Y. Zhang, S. F. Bellon, Discovery and optimization of triazolopyridazines as potent and selective inhibitors of the c-Met kinase, *J. Med. Chem.* **2008**, 51, 2879-2882.

[33] X. Liu, J. Kou, Z. Xiao, F. Tian, J. Hu, P. Zheng, W. Zhu, Design, Synthesis and Biological Evaluation of 6,7-Disubstituted-4-phenoxyquinoline Derivatives Bearing Pyridazinone Moiety as c-Met Inhibitors. *Molecules.* **2018**, 23, 1543-1560.

Dear editor,

We would like to submit the enclosed manuscript entitled "**Discovery of Novel c-Mesenchymal-Epithelia Transition Factor (c-Met) and Histone Deacetylase (HDAC) Dual Inhibitors**", which we wish to be considered for publication in "European Journal of Medicinal Chemistry". No conflict of interest exits in the submission of this manuscript, and manuscript is approved by all authors for publication. I would like to declare on behalf of my co-authors that the work described was our original research that has not been published previously and not under consideration for publication elsewhere, in whole or in part. All the authors listed have approved the manuscript that is enclosed.